measurement of β-cell mass is presently possible only by autopsy. It has recently been reported that antagonistic probes as well as agonistic probes are useful for molecular imaging by targeting peptide receptors [18]. In the present study, we demonstrate for the first time that the GLP-1R antagonist exendin(9-39) is a potential probe for the imaging of pancreatic β-cells.

Acknowledgments

We thank Dr. M. Hara, University of Chicago, for generously providing us transgenic MIP-GFP mice. This work was supported by a Research Grant on Nanotechnical Medicine from the Ministry of Health, Labour, and Welfare of Japan, and by Scientific Research Grants from the Ministry of Education, Culture, Sports, Science, and Technology of Japan, and also by Kyoto University Global COE Program "Center for Frontier Medicine".

References

[1] W.V. Tamborlane, W. Bonfig, E. Boland, Recent advances in treatment of youth with type 1 diabetes: better care through technology, Diabet. Med. 18 (2001) 864–870.
[2] L. Groop, Pathogenesis of type 2 diabetes: the relative contribution of insulin resistance and impaired insulin secretion, Int. J. Clin. Pract. Suppl. (2000) 3–13.
[3] H. Sakuraba, H. Mizukami, N. Yagihashi, R. Wada, C. Hanyu, S. Yagihashi, Reduced beta-cell mass and expression of oxidative stress-related DNA damage in the islet of Japanese type II diabetic patients, Diabetologia 45 (2002) 85–96.
[4] A.E. Butler, J. Janson, S. Bonner-Weir, R. Ritzel, R.A. Rizza, P.C. Butler, Beta-cell deficit and increased beta-cell apoptosis in humans with type 2 diabetes, Diabetes 52 (2003) 102–110.
[5] K.H. Yoon, S.H. Ko, J.H. Cho, J.M. Lee, Y.B. Ahn, K.H. Song, S.J. Yoo, M.I. Kang, B.Y. Cha, K.W. Lee, H.Y. Son, S.K. Kang, H.S. Kim, I.K. Lee, S. Bonner-Weir, Selective beta-cell loss and alpha-cell expansion in patients with type 2 diabetes mellitus in Korea, J. Clin. Endocrinol. Metab. 88 (2003) 2300–2308.
[6] J. Rahier, Y. Guiot, R.M. Goebbels, C. Sempoux, J.C. Henquin, Pancreatic beta-cell mass in European subjects with type 2 diabetes, Diabetes Obes. Metab. 10 (Suppl. 4) (2008) 32–42.
[7] S. Schneider, Efforts to develop methods for in vivo evaluation of the native beta-cell mass, Diabetes Obes. Metab. 10 (Suppl. 4) (2008) 109–118.
[8] L.L. Baggio, D.J. Drucker, Biology of incretins: GLP-1 and GIP, Gastroenterology 132 (2007) 2131–2157.
[9] J.J. Holst, The physiology of glucagon-like peptide 1, Physiol. Rev. 87 (2007) 1409–1439.
[10] J. Eng, W.A. Kleinman, L. Singh, G. Singh, J.P. Raufman, Isolation and characterization of exendin-4, an exendin-3 analogue, from *Heloderma suspectum* venom. Further evidence for an exendin receptor on dispersed acini from guinea pig pancreas, J. Biol. Chem. 267 (1992) 7402–7405.
[11] R. Goke, H.C. Fehmann, T. Linn, H. Schmidt, M. Krause, J. Eng, B. Goke, Exendin-4 is a high potency agonist and truncated exendin-(9-39)-amide an antagonist at the glucagon-like peptide 1-(7-36)-amide receptor of insulin-secreting beta-cells, J. Biol. Chem. 268 (1993) 19650–19655.
[12] M. Hara, X. Wang, T. Kawamura, V.P. Bindokas, R.F. Dizon, S.Y. Alcoser, M.A. Magnuson, G.I. Bell, Transgenic mice with green fluorescent protein-labeled pancreatic beta-cells, Am. J. Physiol. Endocrinol. Metab. 284 (2003) E177–E183.
[13] E. Mukai, H. Ishida, S. Kato, Y. Tsuura, S. Fujimoto, A. Ishida-Takahashi, M. Horie, K. Tsuda, Y. Seino, Metabolic inhibition impairs ATP-sensitive K+ channel block by sulfonylurea in pancreatic beta-cells, Am. J. Physiol. 274 (1998) E38–E44.
[14] R. Sutton, M. Peters, P. McShane, D.W. Gray, P.J. Morris, Isolation of rat pancreatic islets by ductal injection of collagenase, Transplantation 42 (1986) 689–691.
[15] S. Al-Sabah, D. Donnelly, A model for receptor-peptide binding at the glucagon-like peptide-1 (GLP-1) receptor through the analysis of truncated ligands and receptors, Br. J. Pharmacol. 140 (2003) 339–346.
[16] M. Gotthardt, G. Lalyko, J. van Eerd-Vismale, B. Keil, T. Schurrat, M. Hower, P. Laverman, T.M. Behr, O.C. Boerman, B. Goke, M. Behe, A new technique for in vivo imaging of specific GLP-1 binding sites: first results in small rodents, Regul. Pept. 137 (2006) 162–167.
[17] S.E. Kahn, D.B. Carr, M.V. Faulenbach, K.M. Utzschneider, An examination of beta-cell function measures and their potential use for estimating beta-cell mass, Diabetes Obes. Metab. 10 (Suppl. 4) (2008) 63–76.
[18] M. Schottelius, H.J. Wester, Molecular imaging targeting peptide receptors, Methods 48 (2009) 161–177.

Life Sciences 84 (2009) 876–881

Contents lists available at ScienceDirect

Life Sciences

journal homepage: www.elsevier.com/locate/lifescie

Effects of long-term dipeptidyl peptidase-IV inhibition on body composition and glucose tolerance in high fat diet-fed mice

Xibao Liu [a], Norio Harada [a], Shunsuke Yamane [a], Lisa Kitajima [b], Saeko Uchida [b], Akihiro Hamasaki [a], Eri Mukai [a,c], Kentaro Toyoda [a], Chizumi Yamada [a], Yuichiro Yamada [a,d], Yutaka Seino [a,e], Nobuya Inagaki [a,f,*]

[a] Department of Diabetes and Clinical Nutrition, Graduate School of Medicine, Kyoto University, Kyoto, Japan
[b] Molecular Function and Pharmacology Laboratories, Taisho Pharmaceutical Co., Ltd., Saitama, Japan
[c] Japan Association for the Advancement of Medical Equipment, Tokyo, Japan
[d] Department of Endocrinology and Diabetes and Geriatric Medicine, Akita University School of Medicine, Akita, Japan
[e] Kansai Electric Power Hospital, Osaka, Japan
[f] CREST of Japan Science and Technology Cooperation (JST), Kyoto, Japan

ARTICLE INFO

Article history:
Received 10 February 2009
Accepted 28 March 2009

Keywords:
Dipeptidyl peptidase-IV (DPP-IV)
DPP-IV inhibitor
Incretin
Glucagon-like peptide-1 (GLP-1)
Gastric inhibitory polypeptide (GIP)

ABSTRACT

Aim: Glucagon-like peptide-1 (GLP-1) and gastric inhibitory polypeptide (GIP) are major incretins associated with body weight regulation. Dipeptidyl peptidase-IV (DPP-IV) inhibitor increases plasma active GLP-1 and GIP. However, the magnitude of the effects of enhanced GLP-1 and GIP signaling by long-term DPP-IV inhibition on body weight and insulin secretion has not been determined. In this study, we compared the effects of long-term DPP-IV inhibition on body composition and insulin secretion of high fat diet (HFD)-fed wild-type (WT) and GLP-1R knockout (*GLP-1R*$^{-/-}$) mice.
Main methods: HFD-fed WT and *GLP-1R*$^{-/-}$ mice were treated with or without DPP-IV inhibitor by drinking water. Food and water intake and body weight were measured during 8 weeks of study. CT-based body composition analysis, Oral glucose tolerance test (OGTT), batch incubation study for insulin secretion and quantitative RT-PCR for expression of incretin receptors in isolated islets were performed at the end of study.
Key findings: DPP-IV inhibitor had no effect on food and water intake and body weight, but increased body fat mass in *GLP-1R*$^{-/-}$ mice. DPP-IV inhibitor-treated WT and *GLP-1R*$^{-/-}$ mice both showed increased insulin secretion in OGTT. In isolated islets of DPP-IV inhibitor-treated WT and *GLP-1R*$^{-/-}$ mice, glucose-induced insulin secretion was increased and insulin secretion in response to GLP-1 or GIP was preserved, without downregulation of incretin receptor expression.
Significance: Long-term DPP-IV inhibition may maintain body composition through counteracting effects of GLP-1 and GIP while improving glucose tolerance by increasing glucose-induced insulin secretion through the synergistic effects of GLP-1 and GIP.

© 2009 Elsevier Inc. All rights reserved.

Introduction

Oral glucose administration leads to much greater insulin release than the equivalent intravenous glucose challenge. Gut hormonal substances released in response to glucose include the incretins glucagon-like peptide-1 (GLP-1) and gastric inhibitory polypeptide /glucose-dependent insulinotropic peptide (GIP), which are responsible for ~50% of postprandial insulin release. GLP-1 and GIP potentiate glucose-induced insulin secretion from pancreatic β-cells by binding their respective receptors and subsequently increasing the intracellular cAMP concentration. In addition to their action on the enteroinsular axis, GLP-1 inhibits glucagon secretion (Komatsu et al. 1989), delays gastric emptying (Willms et al. 1996), decreases body weight through suppression of appetite (Turton et al. 1996), and suppresses β-cell apoptosis (Toyoda et al. 2008), while GIP enhances energy storage in adipocytes (Miyawaki et al. 2002) and calcium accumulation in bone (Tsukiyama et al. 2006). Thus, the incretins are associated with various systems of metabolic homeostasis, including that of both glucose and body weight.

However, the effects of GLP-1 and GIP are limited by their short half-life of a few minutes, which is primarily due to the action of dipeptidyl peptidase-IV (DPP-IV). DPP-IV is an enzyme distributed throughout the body including plasma and the endothelial lining of several organs, and cleaves two amino acids of biologically active peptides including GLP-1 and GIP by recognizing proline or alanine in the second N-terminal amino acid. The resulting N-terminal-truncated forms of GLP-1 and GIP are devoid of bioactivity. Since DPP-IV-deficient rodents show improved glucose tolerance and increased insulin secretion with elevated plasma active GLP-1 levels after oral glucose loading (Marguet et al. 2000; Nagakura et al. 2001), DPP-IV inhibitor and DPP-IV-resistant GLP-1

* Corresponding author. Department of Diabetes and Clinical Nutrition, Graduate School of Medicine, Kyoto University, 54 Shogoin Kawahara-cho, Sakyo-ku, Kyoto 606-8507, Japan. Tel.: +81 75 751 3560; fax: +81 75 751 4244.
E-mail address: inagki@metab.kuhp.kyoto-u.ac.jp (N. Inagaki).

0024-3205/$ – see front matter © 2009 Elsevier Inc. All rights reserved..
doi:10.1016/j.lfs.2009.03.022

receptor agonist are potential targets for the treatment of type 2 diabetes mellitus as a new class of antidiabetic agent. GLP-1 receptor agonist both increases insulin secretion and improves glucose tolerance and decreases body weight in rodents and humans (Szayna et al. 2000; Buse et al. 2004). DPP-IV inhibitor also increases insulin secretion and improves glucose tolerance, but its effect on body weight is controversial (Pospisilik et al. 2002; Lamont and Drucker 2008; Reimer et al. 2002; Ahrén et al. 2002). It is reported that DPP-IV inhibitor do not increase insulin secretion after glucose loading in GLP-1 receptor (GLP-1R)/GIP receptor (GIPR) double knockout (DIRKO) mice, indicating that both GLP-1 and GIP are critically involved in the insulinotropic action of long-term DPP-IV inhibition (Flock et al. 2007). However, the magnitude of the effects of enhanced GLP-1 and GIP signaling by long-term DPP-IV inhibition on body weight and insulin secretion has not been determined.

In the present study, we investigated the long-term effects of DPP-IV inhibition on body composition and insulin secretion using high fat diet (HFD)-fed wild-type (WT) and GLP-1R knockout (*GLP-1R*$^{-/-}$) mice.

Materials and methods

Animals

Mice (C57BL/6 background) were housed under a light/dark cycle of 12 h with free access to food and water. As ingestion of a meal rich in fat is a strong stimulus of incretin signaling (Harada et al. 2008), male WT and *GLP-1R*$^{-/-}$ mice were fed a high fat diet (45% fat, 20% protein and 35% carbohydrate by energy) from 7 weeks of age. Groups of treated HFD-fed WT and *GLP-1R*$^{-/-}$ mice received DPP-IV inhibitor in drinking water (0.5% W/V), while groups of untreated HFD-fed WT and *GLP-1R*$^{-/-}$ mice received drinking water without DPP-IV inhibitor. All the *GLP-1R*$^{-/-}$ mice were genotyped by Southern blot analysis. The DPP-IV inhibitor, provided by Taisho Pharmaceutical Co., Ltd., showed an inhibitory action on DPP-IV enzymatic activity against substrate H-Gly-Pro-7-amino-4-methyl coumarin (Gly-Pro-AMC) with IC_{50} (half maximal inhibitory concentration) of 0.0046 uM (Fukushima et al. 2008), while its IC_{50} on DPP-8 and DPP-9 were only 1.34 uM and 0.527 uM, respectively (unpublished data). Throughout the 8 weeks of study, water and food intake and body weight were measured once every 3 days. All mice care and procedures were approved by the Animal Care Committee of Kyoto University.

CT-based body composition analysis

The WT and *GLP-1R*$^{-/-}$ mice treated with or without DPP-IV inhibitor for 8 weeks were anesthetized and scanned along the body axis using LaTheta (LCT-100M) experimental animal CT system (Aloka, Tokyo, Japan). Contiguous 1-mm slice images of the whole abdominal cavity were used for quantitative assessment using LaTheta software (version 1.00). Weights of total fat mass, which comprises visceral fat mass and subcutaneous fat mass, and lean mass were quantitatively evaluated.

Oral glucose tolerance test (OGTT)

The WT and *GLP-1R*$^{-/-}$ mice treated with or without DPP-IV inhibitor for 8 weeks were fasted for 16 h and administered glucose (2 g/kg weight body) orally. Blood was collected from the orbital sinus of the mice at the indicated times (0, 15, 30, 60 and 120 min after glucose loading). Blood glucose levels were measured by the enzyme-electrode method. Plasma insulin levels were measured using an ELISA kit (Shibayagi, Gunma, Japan).

Measurement of plasma active GLP-1 levels and DPP-IV activity

For measurement of active GLP-1 levels, blood collected at 15 min after oral glucose loading was mixed with 2% EDTA· 4Na and 1% DPP-IV inhibitor (Linco Research, St Charles, MO). Active GLP-1 levels in plasma obtained by centrifugation (2000× g, 10 min, 4 °C) were measured using an active GLP-1 (7–36) ELISA kit (Linco Research).

Plasma DPP-IV activity was measured using a published method (Fukushima et al. 2008). In brief, 12.5 μl of plasma in duplicate was incubated with 37.5 μl of substrate cocktail (66.7 μM Gly-Pro-AMC, 25 mM HEPES, 140 mM NaCl, 26.6 mM $MgCl_2$, and 1% (w/v) BSA, pH 7.8) in the dark at room temperature for 5 min. The reaction was stopped by addition of 50 μl of 25% (v/v) acetic acid. Fluorescence was measured using a spectrofluorometer at excitation 360 nm/emission 465 nm. A standard curve was drawn using free AMC in standard buffer (25 mM HEPES, 140 mM NaCl, 20 mM $MgCl_2$, 1% (w/v) BSA, pH 7.8). DPP-IV activity (mU) is shown as the AMC (μM) generated in 1 ml plasma for 1 min of reaction time.

Measurement of insulin secretion in isolated islets

Islets were isolated from mice and preincubated at 37 °C for 30 min in 20 ml of Krebs-Ringer bicarbonate buffer (KRBB; 120 mM NaCl, 4.7 mM KCl, 1.2 mM $MgSO_4$, 1.2 mM KH_2PO_4, 2.4 mM $CaCl_2$, 20 mM $NaHCO_3$) supplemented with 10 mM HEPES and 0.2% (w/v) BSA and gassed with a mixture of 95% O_2 and 5% CO_2 (KRBB medium) containing 2.8 mM glucose. 10 size-matched islets collected in each tube were incubated at 37 °C for 30 min in 700 μl of KRBB medium containing 2.8 mM or 11.1 mM glucose with or without incretin peptides (100 nM human GLP-1 or 100 nM human GIP (Peptide Institute, Inc. Osaka, Japan)). Islets were then pelleted by centrifugation (9000× g, 2 min, 4 °C) and aliquots of the buffer were sampled. The amount of immunoreactive insulin was determined by radio-immunoassay (RIA). To determine insulin content, islets were homogenized in 400 μl acid-ethanol (37% HCl in 75% ethanol, 15:1000 (v/v)) and extracted at 4 °C overnight. The acidic extracts were dried by vacuum, reconstituted, and subjected to insulin measurement.

Measurement of mRNA expression of GLP-1R and GIPR in isolated islets

Measurement of mRNA expression of GLP-1R and GIPR was performed by quantitative RT-PCR as described previously (Harada et al. 2008). Briefly, total RNA was extracted from isolated islets with RNeasy mini kit (Qiagen, Valencia, CA) and treated with DNase (Qiagen). First strand cDNA was synthesized by SuperScript™ II Reverse Transcriptase system (Invitrogens, Grand Island, NY) according to manufacturer's instructions. SYBER Green PCR Master Mix (Applied Biosystems) was prepared for the PCR run. The PCR included 2 min at 50 °C and 10 min at 90 °C, followed by 50 cycles at 95 °C for 15 s and at 60 °C for 1 minute. The sequences of GLP-1R primers were 5′-CAACCGGACCTTTGATGACTA-3′ and 5′-GCTGTGCAGAACCGGTACAC-3′; the sequences of GIPR primers were 5′-CCTCCACTGGTCCCTACAC-3′ and 5′-GATAAACACCCTCCACCAGTAG-3′; the sequences of GAPDH primers were 5′-AAATGGTGAAGGTCGGTGTG-3′ and 5′-TCGTTGATGGCAACAATCTC-3′.

Statistical analyses

Data are expressed as means ± SE. Statistical analyses were performed by ANOVA and unpaired student's *t* test. *P* values<0.05 were considered significant.

Results

Body weight and body composition of DPP-IV inhibitor-treated HFD-fed mice

Water intake, food intake, and body weight of HFD-fed WT and *GLP-1R*$^{-/-}$ mice with or without DPP-IV inhibitor administration were measured. In WT mice, water and food intake in DPP-IV

inhibitor-treated and untreated mice were similar during the 8 weeks of the study (Fig. 1A). In *GLP-1R*$^{-/-}$ mice, water and food intake in DPP-IV inhibitor-treated and untreated mice also were similar (Fig. 1A). A significant difference in body weight between DPP-IV inhibitor-untreated WT and *GLP-1R*$^{-/-}$ mice appeared from the 36th day (30.9 ± 1.3 g vs. 27.0 ± 0.6 g, $P<0.05$) (Fig. 1B). Body weight of WT mice and *GLP-1R*$^{-/-}$ mice was unaffected by DPP-IV inhibitor treatment during the 8 weeks of the study. To measure the effect of DPP-IV inhibitor on body composition, CT-based analysis was performed (Fig. 1C). In WT mice, there was no significant difference in body fat ratio between DPP-IV inhibitor-treated and untreated mice. However, the body fat ratio of DPP-IV inhibitor-treated *GLP-1R*$^{-/-}$ mice was significantly increased compared with that of untreated *GLP-1R*$^{-/-}$ mice (44.13 ± 1.55 vs. 32.60 ± 3.50, $P<0.05$).

OGTT of DPP-IV inhibitor-treated mice

In OGTT, blood glucose levels at 30 and 60 min were significantly lower in DPP-IV inhibitor-treated WT and *GLP-1R*$^{-/-}$ mice compared to those in untreated WT and *GLP-1R*$^{-/-}$ mice, respectively (Fig. 2A). In WT mice, the plasma insulin level of DPP-IV inhibitor-treated mice was 2.3 times higher at 15 min than that of untreated control mice ($P<0.05$), while in *GLP-1R*$^{-/-}$ mice, the plasma insulin levels of DPP-IV inhibitor-treated mice were 1.6 and 1.4 times higher at 15 and 30 min than those of untreated control mice, respectively ($P<0.05$) (Fig. 2B). In addition, the plasma insulin level of DPP-IV inhibitor-treated WT mice was 1.6 times higher at 15 min compared with that of DPP-IV inhibitor-treated *GLP-1R*$^{-/-}$ mice ($P<0.05$) (Fig. 2B).

We also measured plasma DPP-IV activity and active GLP-1 levels in WT and *GLP-1R*$^{-/-}$ mice at 15 min by OGTT. 75–80% of plasma DPP-IV activity in both untreated WT and *GLP-1R*$^{-/-}$ mice was inhibited by DPP-IV inhibitor treatment (Fig. 2C). Plasma levels of active GLP-1 were significantly elevated in DPP-IV inhibitor-treated WT and *GLP-1R*$^{-/-}$ mice compared to those in the respective untreated mice (Fig. 2D).

Insulin secretion and incretin receptor expression of islets isolated from DPP-IV inhibitor-treated mice

To determine insulin secretion in response to glucose and GLP-1 and GIP, batch incubation experiments were performed using islets isolated from WT and *GLP-1R*$^{-/-}$ mice after 8 weeks of treatment (Fig. 3A). In islets of WT mice, insulin secretion in response to 2.8 mM glucose was similar in DPP-IV inhibitor-treated and untreated mice. However, insulin secretion in response to 11.1 mM glucose, 11.1 mM glucose with GLP-1, and 11.1 mM glucose with GIP was significantly higher in DPP-IV inhibitor-treated mice than those in untreated mice. In addition, both GLP-1 and GIP augmented insulin secretion in the presence of 11.1 mM glucose in both DPP-IV inhibitor-treated and untreated mice. In islets of *GLP-1R*$^{-/-}$ mice, as in those of WT mice, insulin secretion in response to 2.8 mM glucose was similar in DPP-IV inhibitor-treated and untreated mice, and insulin secretion in response to 11.1 mM glucose, 11.1 mM glucose with GLP-1, and 11.1 mM glucose with GIP was significantly higher in DPP-IV inhibitor-treated mice than those in untreated mice. However, in *GLP-1R*$^{-/-}$ mice, potentiation of insulin secretion by incretin in the presence of 11.1 mM glucose was observed only by GIP and not by GLP-1 in both DPP-IV inhibitor-treated and untreated mice. Insulin content was similar among all groups of mice (data not shown).

To determine the effect of DPP-IV inhibitor treatment on the mRNA expression of GLP-1R and GIPR in islets, we performed quantitative RT-PCR after 8 weeks of study (Fig. 3B). The mRNA expression levels of GLP-1R and GIPR in DPP-IV inhibitor-treated and untreated WT mice were similar, as were total mRNA expression levels of GIPR in DPP-IV inhibitor-treated and untreated *GLP-1R*$^{-/-}$ mice.

Discussion

In the present study, we evaluated body composition and glucose control in the absence of the GLP-1 signaling using *GLP-1R*$^{-/-}$ mice treated with DPP-IV inhibitor for 8 weeks to clarify GLP-1 and GIP action under long-term DPP-IV inhibition.

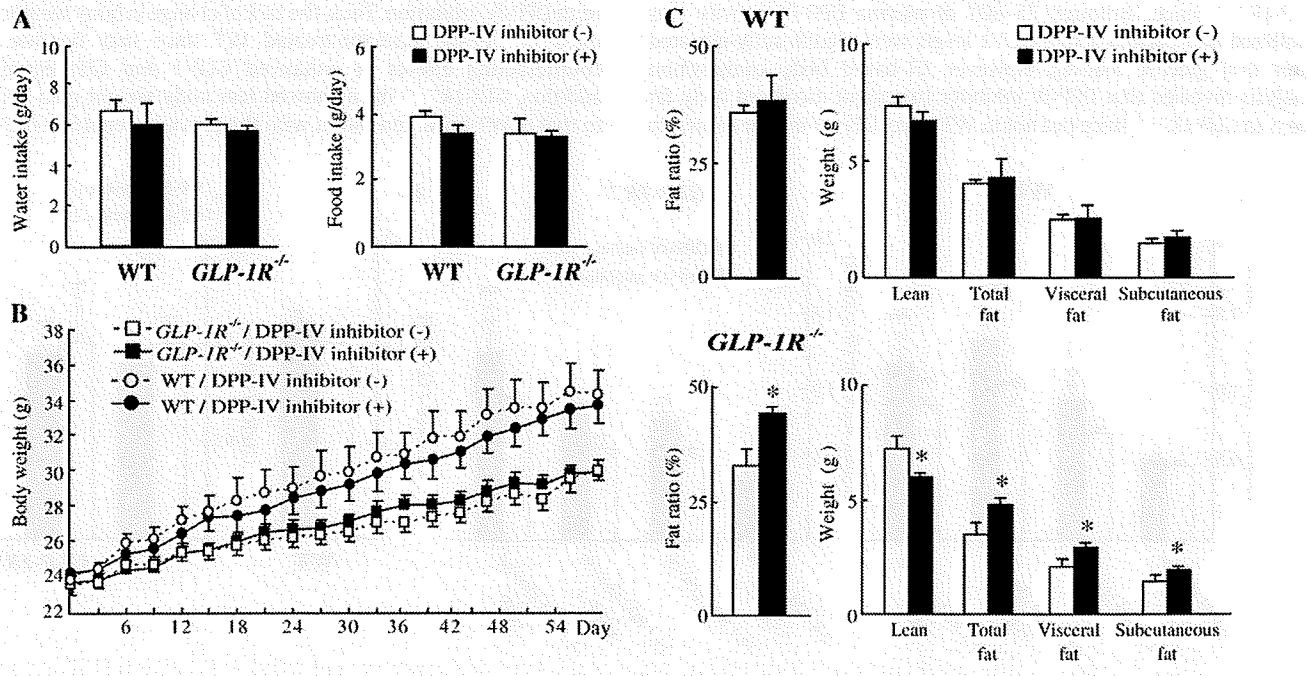

Fig. 1. Water and food intake, body weight and CT-based body composition analysis. (A) Water intake (left) and food intake (right) of WT and *GLP-1R*$^{-/-}$ mice treated with (filled) or without (open) DPP-IV inhibitor at the last week of study (average of 1 day). (B) Body weight change of WT (circle) and *GLP-1R*$^{-/-}$ (square) mice treated with (filled) or without (open) DPP-IV inhibitor. (C) CT-based body composition analysis of WT (upper) and *GLP-1R*$^{-/-}$ (lower) mice treated with (filled) or without (open) DPP-IV inhibitor. Fat ratio calculated as: total fat/(lean + total fat) × 100. Values are means ± SE. *$P<0.05$ vs. untreated mice ($n=5$–6).

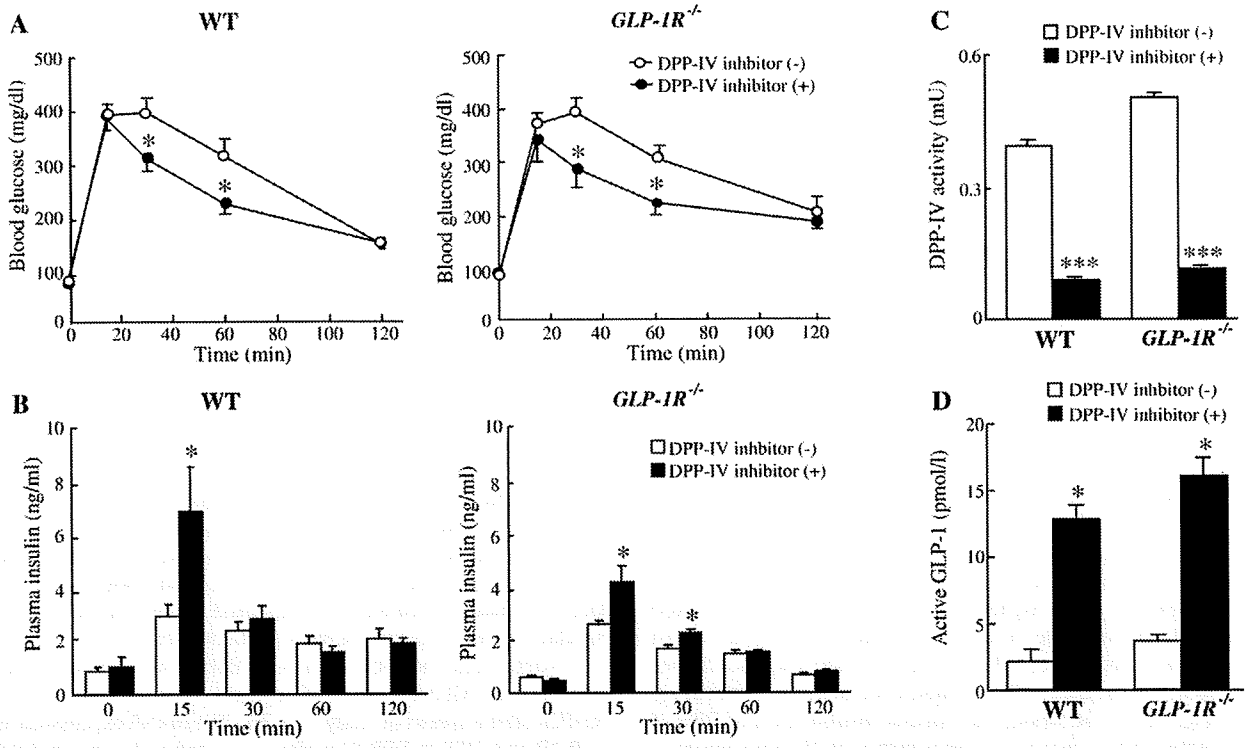

Fig. 2. OGTT. Blood glucose levels (A) and plasma insulin levels (B) of WT (left) and *GLP-1R*$^{-/-}$ (right) mice treated with (filled) or without (open) DPP-IV inhibitor after 8 weeks of study. Plasma DPP-IV activity (C) and plasma levels of active GLP-1 (D) at 15 min for WT and *GLP-1R*$^{-/-}$ mice treated with (filled) or without (open) DPP-IV inhibitor. Values are means ± SE. **P*<0.05, ****P*<0.001 vs. untreated mice (n = 5–6).

HFD-fed DPP-IV-deficient rodents exhibit reduced food intake and resistance to development of obesity with elevated active GLP-1 levels (Yasuda et al. 2002; Conarello et al. 2003), and DPP-IV inhibitor has been shown to reduce body weight in some previous studies using rodent models (Pospisilik et al. 2002; Lamont and Drucker 2008). In the present study, no alteration in body weight was found after 8 weeks of DPP-IV inhibitor treatment either in HFD-fed WT or *GLP-1R*$^{-/-}$ mice, although 75–80% of plasma DPP-IV activity was inhibited and plasma active GLP-1 levels were significantly elevated after oral glucose loading. However, CT-based body composition analysis revealed that DPP-IV inhibitor treatment increased body fat mass in *GLP-1R*$^{-/-}$ mice but not in WT mice. DPP-IV is well known to be involved in inactivation of both GLP-1 and GIP, and plasma active GIP levels are elevated by treatment of DPP-IV inhibitor (Deacon et al. 2001). The receptor for GIP, differently from that for GLP-1, is expressed in adipocytes, and GIP directly facilitates energy accumulation in adipose tissue (Miyawaki et al. 2002; Naitoh et al. 2008). Our results suggest that fat accumulation is potentiated by fat-augmenting factors including GIP in the absence of the GLP-1 signaling under long-term DPP-IV inhibition. Thus, the lack of change in body weight and fat mass in DPP-IV inhibitor-treated WT mice may be due to the counteracting effects of enhanced GLP-1 and GIP signaling. In addition, *GLP-1R*$^{-/-}$ mice showed less body weight gain compared to that of WT mice, consistent with the previous report on *GLP-1R*$^{-/-}$

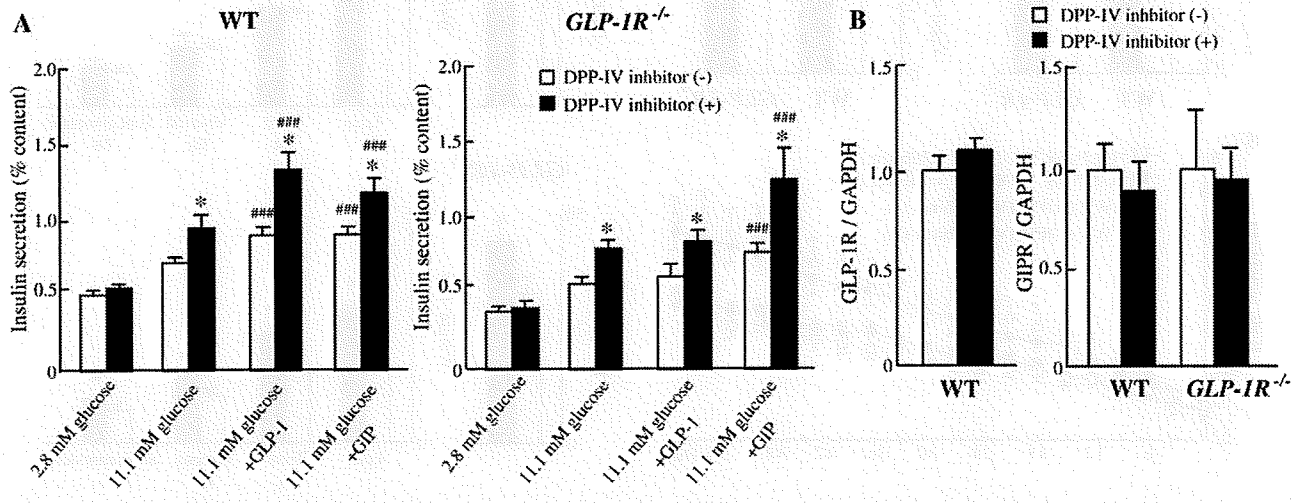

Fig. 3. Functional study of isolated islets. (A) Insulin secretion from islets isolated from WT (left) and *GLP-1R*$^{-/-}$ (right) mice treated with (filled) or without (open) DPP-IV inhibitor after 8 weeks of study. Values are means ± SE. **P*<0.05 vs. untreated mice. ###*P*<0.05 vs. 11.1 mM glucose. (B) The mRNA expression of GLP-1R and GIPR in islets isolated from WT and *GLP-1R*$^{-/-}$ mice treated with (filled) or without (open) DPP-IV inhibitor. GLP-1R and GIPR mRNA levels were corrected for GAPDH mRNA levels, respectively. Data of DPP-IV inhibitor-treated mice is shown relative to untreated mice. Values are means ± SE. (n = 5–8).

mice showing reduced body weight gain compared to that of WT mice, possibly due to enhanced locomotor activity and increased energy expenditure (Hansotia et al. 2007).

GLP-1 and GIP both are clearly involved in the effects of long-term DPP-IV inhibition on improved glucose tolerance, as DPP-IV inhibitor fails to increase insulin secretion and decrease plasma glucose after oral glucose loading in DIRKO mice (Flock et al. 2007). Our comparison in the present study of *GLP-1R*$^{-/-}$ mice and WT mice enables us to estimate the magnitude of the effects of enhanced GLP-1 and GIP by long-term DPP-IV inhibition on insulin secretion separately. Improved glucose tolerance and increased plasma insulin with elevated active GLP-1 levels were found in both DPP-IV inhibitor-treated WT and *GLP-1R*$^{-/-}$ mice by OGTT, indicating that GIP contributes to the insulinotropic effects of long-term DPP-IV inhibition in *GLP-1R*$^{-/-}$ mice. Moreover, blood insulin at 15 min in DPP-IV inhibitor-treated *GLP-1R*$^{-/-}$ mice was about half of that in DPP-IV inhibitor-treated WT mice. These results confirm that GLP-1 and GIP are important mediators of the insulinotropic effects of long-term DPP-IV inhibition. In addition, insulin secretion from islets in response to 11.1 mM glucose was increased in DPP-IV inhibitor-treated WT and *GLP-1R*$^{-/-}$ mice, indicating that glucose sensitivity of insulin secretion is augmented by long-term DPP-IV inhibitor administration unrelated to the GLP-1 signaling. However, the mechanism is not known. A recent report found that the glucose sensitivity of insulin secretion in isolated islets of mice improved after GLP-1 receptor agonist treatment due to augmented cAMP-induced activation of protein kinase A (PKA) through the GLP-1 receptor (Winzell and Ahrén 2008). It also was reported that activated PKA due to GLP-1 signaling increased expression of transcription factor pancreatic-duodenum homeobox-1 (PDX-1), translocation of PDX-1 from cytoplasm to nucleus, and phosphorylation of glucose transporter type 2 (GLUT2) in β-cells (Wang et al. 2001; Thorens et al. 1996). Thus, the increased glucose sensitivity of insulin secretion in islets unrelated to the GLP-1 signaling may be the result of augmented GIP signaling due long-term DPP-IV inhibition through similar mechanisms. Further study is required to clarify the augmentation of glucose sensitivity of islets after long-term DPP-IV inhibitor administration.

In addition to the plasma active incretin level, the expression of incretin receptors in islets also influences their insulinotropic effect (Lynn et al. 2001; Xu et al. 2007). Indeed, it has been reported that continuous GLP-1 stimulation results in desensitization of GLP-1R, which can subsequently reduce insulin secretion in response to GLP-1 in insulin-secreting cell lines (Widmann et al. 1996; Green et al. 2005). However, the expression of GLP-1R and GIPR in islets did not change in DPP-IV inhibitor-treated mice in the present study. Furthermore, insulin secretion in response to incretins was maintained in the islets of DPP-IV inhibitor-treated mice, demonstrating that sensitivity of the incretin receptors did not decrease even after 8 weeks of continuous incretin stimulation. These results suggest that the action of DPP-IV inhibitor in glucose control is preserved during long-term DPP-IV inhibitor administration.

Conclusion

Long-term DPP-IV inhibition does not alter body composition, possibly due to the counteracting effects of enhanced GLP-1 and GIP, but does improve glucose tolerance through the synergistic insulinotropic effects of enhanced GLP-1 and GIP, as well as by improved glucose responsiveness in pancreatic islets.

Acknowledgments

We thank Dr. Daniel. J. Drucker (Department of Medicine, The Banting and Best Diabetes Centre, Toronto General Hospital, University of Toronto, Toronto, Canada) for providing the *GLP-1R*$^{-/-}$ mice.

The funding of this study was supported by Scientific Research Grants from the Ministry of Education, Culture, Sports, Science, and Technology (Japan) and from the Ministry of Health, Labor, and Welfare (Japan).

References

Ahrén B, Simonsson E, Larsson H, Landin-Olsson M, Torgeirsson H, Jansson PA, Sandqvist M, Båvenholm P, Efendic S, Eriksson JW, Dickinson S, Holmes D. Inhibition of dipeptidyl peptidase IV improves metabolic control over a 4-week study period in type 2 diabetes. Diabetes Care 25 (5), 869–875, 2002.

Buse JB, Henry RR, Han J, Kim DD, Fineman MS, Baron AD. Exenatide-113 Clinical Study Group. Effects of Exenatide (Exendin-4) on glycemic control over 30 weeks in sulfonylurea-treated patients with type 2 diabetes. Diabetes Care 27 (11), 2628–2635, 2004.

Conarello SL, Li Z, Ronan J, Roy RS, Zhu L, Jiang G, Liu F, Woods J, Zycband E, Moller DE, Thornberry NA, Zhang BB. Mice lacking dipeptidyl peptidase IV are protected against obesity and insulin resistance. Proceedings of the National Academy of Sciences of the United States of America 100 (11), 6825–6830, 2003.

Deacon CF, Danielsen P, Klarskov L, Olesen M, Holst JJ. Dipeptidyl peptidase IV inhibition reduces the degradation and clearance of GIP and potentiates its insulinotropic and antihyperglycemic effects in anesthetized pigs. Diabetes 50 (7), 1588–1597, 2001.

Flock G, Baggio LL, Longuet C, Drucker DJ. Incretin receptors for glucagon-like peptide 1 and glucose-dependent insulinotropic polypeptide are essential for the sustained metabolic actions of Vildagliptin in mice. Diabetes 56 (12), 3006–3013, 2007.

Fukushima H, Hiratate A, Takahashi M, Mikami A, Saito-Hori M, Munetomo E, Kitano K, Chonan S, Saito H, Suzuki A, Takaoka Y, Yamamoto K. Synthesis and structure–activity relationships of potent 4-fluoro-2-cyanopyrrolidine dipeptidyl peptidase IV inhibitors. Bioorganic & Medicinal Chemistry 16 (7), 4093–4106, 2008.

Green BD, Liu HK, McCluskey JT, Duffy NA, O'Harte FP, McClenaghan NH, Flatt PR. Function of a long-term, GLP-1-treated, insulin-secreting cell line is improved by preventing DPP IV-mediated degradation of GLP-1. Diabetes, Obesity & Metabolism 7 (5), 563–569, 2005.

Hansotia T, Maida A, Flock G, Yamada Y, Tsukiyama K, Seino Y, Drucker DJ. Extrapancreatic incretin receptors modulate glucose homeostasis, body weight, and energy expenditure. The Journal of Clinical Investigation 117 (1), 143–152, 2007.

Harada N, Yamada Y, Tsukiyama K, Yamada C, Nakamura Y, Mukai E, Hamasaki A, Liu X, Toyoda K, Seino Y, Inagaki N. A novel gastric inhibitory polypeptide (GIP) receptor splice variant influences GIP sensitivity of pancreatic {beta}-cells in obese mice. American Journal of Physiology. Endocrinology and Metabolism 294 (1), E61–E68, 2008.

Komatsu R, Matsuyama T, Namba M, Watanabe N, Itoh H, Kono N, Tarui S. Glucagonostatic and insulinotropic action of glucagon-like peptide-1-(7-36) amide. Diabetes 38 (7), 902–905, 1989.

Lamont BJ, Drucker DJ. Differential antidiabetic efficacy of incretin agonists versus DPP-4 inhibition in high fat-fed mice. Diabetes 57 (1), 190–198, 2008.

Lynn FC, Pamir N, Ng EH, McIntosh CH, Kieffer TJ, Pederson RA. Defective glucose-dependent insulinotropic polypeptide receptor expression in diabetic fatty zucker rats. Diabetes 50 (5), 1004–1011, 2001.

Marguet D, Baggio L, Kobayashi T, Bernard AM, Pierres M, Nielsen PF, Ribel U, Watanabe T, Drucker DJ, Wagtmann N. Enhanced insulin secretion and improved glucose tolerance in mice lacking CD26. Proceedings of the National Academy of Sciences of the United States of America 97 (12), 6874–6879, 2000.

Miyawaki K, Yamada Y, Ban N, Ihara Y, Tsukiyama K, Zhou H, Fujimoto S, Oku A, Tsuda K, Toyokuni S, Hiai H, Mizunoya W, Fushiki T, Holst JJ, Makino M, Tashita A, Kobara Y, Tsubamoto Y, Jinnouchi T, Jomori T, Seino Y. Inhibition of gastric inhibitory polypeptide signaling prevents obesity. Nature Medicine 8 (7), 738–742, 2002.

Nagakura T, Yasuda N, Yamazaki K, Ikuta H, Yoshikawa S, Asano O, Tanaka I. Improved glucose tolerance via enhanced glucose-dependent insulin secretion in dipeptidyl peptidase IV-deficient Fischer rats. Biochemical and Biophysical Research Communications 284 (2), 501–506, 2001.

Naitoh R, Miyawaki K, Harada N, Mizunoya W, Toyoda K, Fushiki T, Yamada Y, Seino Y, Inagaki N. Inhibition of GIP signaling modulates adiponectin levels under high-fat diet in mice. Biochemical and Biophysical Research Communications 376 (1), 21–25, 2008.

Pospisilik JA, Stafford SG, Demuth HU, Brownsey R, Parkhouse W, Finegood DT, McIntosh CH, Pederson RA. Long-term treatment with the dipeptidyl peptidase IV inhibitor P32/98 causes sustained improvements in glucose tolerance, insulin sensitivity, hyperinsulinemia, and β-cell glucose responsiveness in VDF (fa/fa) zucker rats. Diabetes 51 (4), 943–950, 2002.

Reimer MK, Holst JJ, Ahrén B. Long-term inhibition of dipeptidyl peptidase IV improves glucose tolerance and preserves islet function in mice. European Journal of Endocrinology/European Federation of Endocrine Societies 146 (5), 717–727, 2002.

Szayna M, Doyle ME, Betkey JA, Holloway HW, Spencer RG, Greig NH, Egan JM. Exendin-4 decelerates food intake, weight gain, and fat deposition in Zucker rats. Endocrinology 141 (6), 1936–1941, 2000.

Thorens B, Dériaz N, Bosco D, DeVos A, Pipeleers D, Schuit F, Meda P, Porret A. Protein kinase A-dependent phosphorylation of GLUT2 in pancreatic beta cells. The Journal of Biological Chemistry 271 (14), 8075–8081, 1996.

Toyoda K, Okitsu T, Yamane S, Uonaga T, Liu X, Harada N, Uemoto S, Seino Y, Inagaki N. GLP-1 receptor signaling protects pancreatic beta cells in intraportal islet transplant by inhibiting apoptosis. Biochemical and Biophysical Research Communications 367 (4), 793–798, 2008.

Tsukiyama K, Yamada Y, Yamada C, Harada N, Kawasaki Y, Ogura M, Bessho K, Li M, Amizuka N, Sato M, Udagawa N, Takahashi N, Tanaka K, Oiso Y, Seino Y. Gastric

inhibitory polypeptide as an endogenous factor promoting new bone formation after food ingestion. Molecular Endocrinology 20 (7), 1644–1651, 2006.
Turton MD, O'Shea D, Gunn I, Beak SA, Edwards CM, Meeran K, Choi SJ, Taylor GM, Heath MM, Lambert PD, Wilding JP, Smith DM, Ghatei MA, Herbert J, Bloom SR. A role for glucagon-like peptide-1 in the central regulation of feeding. Nature 379 (6560), 69–72, 1996.
Wang X, Zhou J, Doyle ME, Egan JM. Glucagon-like peptide-1 causes pancreatic duodenal homeobox-1 protein translocation from the cytoplasm to the nucleus of pancreatic beta-cells by a cyclic adenosine monophosphate/protein kinase A-dependent mechanism. Endocrinology 142 (5), 1820–1827, 2001.
Widmann C, Dolci W, Thorens B. Desensitization and phosphorylation of the glucagon-like peptide-I (GLP-1) receptor by GLP-1 and 4-Phorbol 12-Myristate 13-Acetate. Molecular Endocrinology 10 (1), 62–75, 1996.
Willms B, Werner J, Holst JJ, Orskov C, Creutzfeldt W, Nauck MA. Gastric emptying, glucose responses, and insulin secretion after a liquid test meal: Effects of exogenous glucagon-like peptide-1 (GLP-1)-(7–36) amide in type 2 (noninsulin-dependent) diabetic patients. The Journal of Clinical Endocrinology and Metabolism 81 (1), 327–332, 1996.
Winzell MS, Ahrén B. Durable islet effects on insulin secretion and protein kinase A expression following exendin-4 treatment of high-fat diet-fed mice. Journal of Molecular Endocrinology 40 (2), 93–100, 2008.
Xu G, Kaneto H, Laybutt DR, Duvivier-Kali VF, Trivedi N, Suzuma K, King GL, Weir GC, Bonner-Weir S. Downregulation of GLP-1 and GIP receptor expression by hyperglycemia: Possible contribution to impaired incretin effects in diabetes. Diabetes 56 (6), 1551–1558, 2007.
Yasuda N, Nagakura T, Yamazaki K, Inoue T, Tanaka I. Improvement of high fat-diet-induced insulin resistance in dipeptidyl peptidase IV-deficient Fischer rats. Life Sciences 71 (2), 227–238, 2002.

Journal of Gastroenterology and Hepatology
JGHF
doi:10.1111/j.1440-1746.2008.05669.x

HEPATOLOGY

SRD5B1 gene analysis needed for the accurate diagnosis of primary 3-oxo-Δ^4-steroid 5β-reductase deficiency

Isao Ueki,* Akihiko Kimura,* Huey-Ling Chen,† Tohru Yorifuji,‡ Jun Mori,§ Susumu Itoh,¶ Kenichi Maruyama,** Takashi Ishige,†† Hajime Takei,‡‡ Hiroshi Nittono,‡‡ Takao Kurosawa,§§ Masayoshi Kage¶¶ and Toyojiro Matsuishi*

*Department of Pediatrics and Child Health, ¶¶Department of Pathology, Kurume University School of Medicine, Kurume, Fukuoka, ‡Department of Pediatrics, Kyoto University, Graduate School of Medicine, Faculty of Medicine, §Department of Pediatrics, Kyoto Prefectural University of Medical Graduate School of Medical Sciences, Kyoto, ¶Department of Pediatrics, Faculty of Medicine, Kagawa University, Kida-gun, Kagawa, **Department of Neonatology, Gunma Children's Medical Center, Shibukawa, ††Department of Pediatrics, Gunma University, Graduate School of Medicine, Maebashi, Gunma, ‡‡Junshin Clinic, Yokohama, Kanagawa, §§Faculty of Pharmaceutical Sciences, Health Sciences University of Hokkaido, Ishikari-Tobetsu, Hokkaido, Japan; and †Department of Pediatrics, National Taiwan University Hospital, Taipei, Taiwan

Key words
3-oxo-Δ^4 bile aciduria, inborn error of bile acid metabolism, mutation analysis, neonatal cholestasis, ursodeoxycholic acid therapy.

Accepted for publication 14 August 2008.

Correspondence
Dr Akihiko Kimura, Department of Pediatrics and Child Health, Kurume University School of Medicine, 67 Asahi-machi, Kurume-shi 830-0011, Japan. Email: hirof@med.kurume-u.ac.jp

Abstract

Background and Aim: We encounter hyper-3-oxo-Δ^4 bile aciduria in patients with severe cholestatic liver disease or fulminant liver failure during the neonatal period. However, simply by bile acid analysis, it is difficult to distinguish hyper-3-oxo-Δ^4 bile aciduria from primary 3-oxo-Δ^4-steroid 5β-reductase deficiency.

Methods: To determine whether 3-oxo-Δ^4-steroid 5β-reductase (*SRD5B1*) gene analysis is required for the accurate diagnosis of 3-oxo-Δ^4-steroid 5β-reductase deficiency, we evaluated the laboratory data, bile acid analysis and *SRD5B1* gene analysis from six patients with hyper-3-oxo-Δ^4 bile aciduria.

Results: Based upon the results, four patients who had developed neonatal liver failure were diagnosed as having neonatal hemochromatosis. Two patients with chronic cholestasis were diagnosed as having primary 3-oxo-Δ^4-steroid 5β-reductase deficiency by *SRD5B1* gene analysis. The *SRD5B1* gene in these two patients had a heterozygous mutation, G737A (Gly 223 Glu) in one patient and C217T (Arg 50 stop) in the other.

Conclusions: Based upon our limited data, we conclude that SDR5B1 gene analysis is required for the accurate diagnosis of 3-oxo-Δ^4-steroid 5β-reductase deficiency. Moreover, we think that it is important to elucidate whether there is a heterozygous or a compound heterozygous mutation of the *SRD5B1* gene in our two patients.

Introduction

We often encounter hyper-3-oxo-Δ^4 bile aciduria in children with severe cholestatic liver disease or fulminant liver failure during the neonatal period.[1–4] When greater than 75% of the total bile acids in the urine of patients with cholestasis consist of 3-oxo-Δ^4 bile acids, 3-oxo-Δ^4-steroid 5β-reductase deficiency should be suspected[5] (Fig. 1). However, using clinical symptoms, such as the absence of pruritus despite the presence of conjugated hyperbilirubinemia, or using laboratory data such as a normal value of γ-glutamyltransferase (GGT) activity, or total bile acid concentration by enzymatic assay using 3α-hydroxysteroid dehydrogenase, or by analysis of bile acids using gas chromatography-mass spectrometry (GC-MS), it is difficult to distinguish primary 3-oxo-Δ^4-steroid 5β-reductase deficiency from a variety of other cholestatic liver diseases causing hyper-3-oxo-Δ^4 bile aciduria. Therefore, we attempted to assess whether it is necessary to carry out gene analysis of 3-oxo-Δ^4-steroid 5β-reductase (SRD5B1 or AKR1D1) on chromosome 7q32-33[6] to establish the diagnosis.

To date, only five patients with primary 3-oxo-Δ^4-steroid 5β-reductase deficiency have been reported in the literature.[7,8] In this disease, if the diagnosis is delayed, primary bile acid treatment cannot be carried out[9,10] and patients suffer a poor clinical outcome as a result.

In the present study, we report the results of *SRD5B1* gene analysis in six patients with hyper-3-oxo-Δ^4 bile aciduria who were recently treated at Kurume, Kyoto, Kagawa, Gunma and Taiwan university hospitals. Moreover, we examined the clinical symptoms, laboratory data and liver histological findings between primary and secondary 3-oxo-Δ^4-steroid 5β-reductase deficiency.

Methods

We evaluated six patients who developed hyper-3-oxo-Δ^4 bile aciduria between August 2002 and July 2007. Their clinical

Journal of Gastroenterology and Hepatology 24 (2009) 776–785 © 2008 The Authors
Journal compilation © 2008 Journal of Gastroenterology and Hepatology Foundation and Blackwell Publishing Asia Pty Ltd

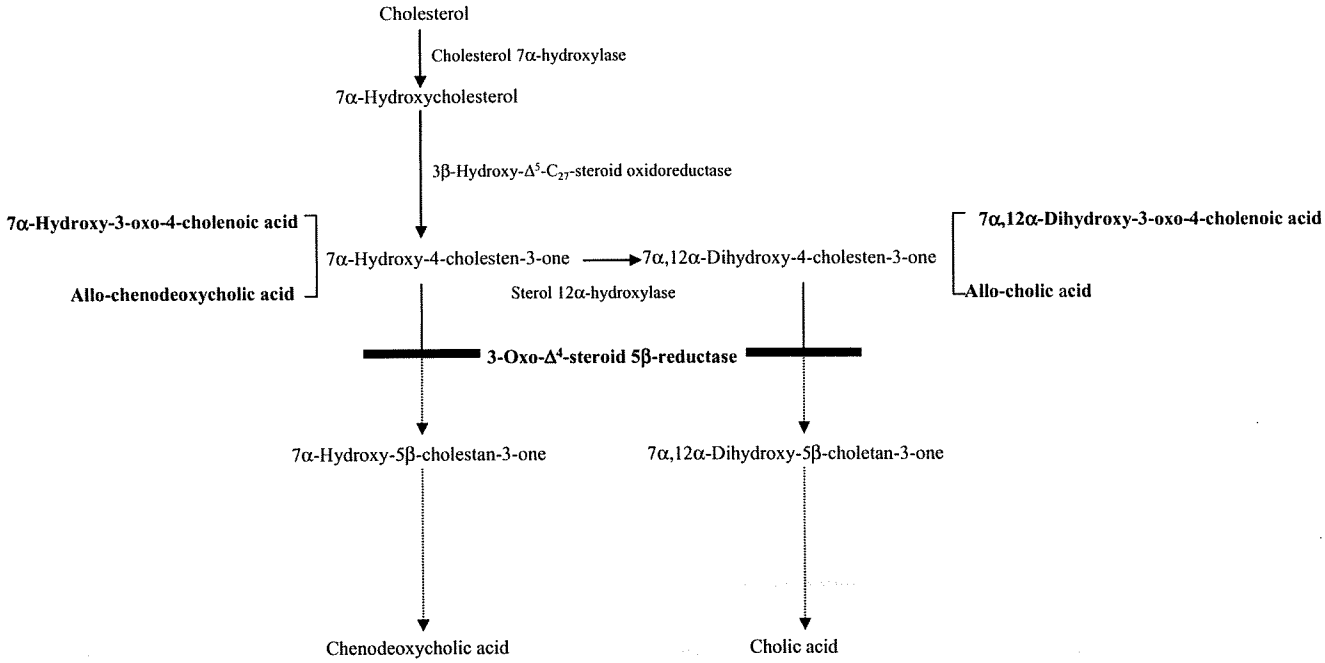

Figure 1 Effect of a defect of 3-oxo-Δ⁴-steroid 5β-reductase. Reduced synthesis of primary bile acids from cholesterol and increased synthesis of 3-oxo-Δ⁴ and allo-bile acids are shown in a flow chart of the classical pathway.

Table 1 Laboratory data of patients with hyper 3-oxo-Δ⁴ bile aciduria on admission

Patient (normal values)	1	2	3	4	5	6
Total bilirubin (0.3–1.5 mg/dL)	11.5	4.9	25.5	11.9	11.3	16.2
Direct bilirubin (<0.6 mg/dL)	6.9	2.0	4.3	4.1	8.3	8.9
Aspartate aminotransferase (13–33 U/L)	29	45	474	1352	934	1180
Alanine aminotransferase (8–42 U/L)	4	6	321	1079	679	878
γ-Glutamyltransferase (10–47 U/L)	36	78	19	17	76	52
Total bile acids (<10 μmol/L)	69.4	28.4	20.4	14.4	2.7	19.8
Serum ammonia (12–66 μg/dL)	270	241	176	187	116	n.d.
Ferritin (male: 23.0–183.0, female: 4.9–96.6 ng/mL)	n.d.	n.d.	18 070	3763	120	n.d.
Prothrombin activity (60–130%)	29	n.d.	7	20	43	n.d.

Prothrombin time in patient 6 was 19.8 s.
n.d., not done.

symptoms, laboratory data, bile acid analysis by GC-MS, and *SRD5B1* gene analysis were analyzed retro- and prospectively.

Case reports

Patient 1

At 35 weeks of gestational age, a Japanese boy was delivered by emergency cesarean section with complications and fetal distress. His birthweight was 1269 g. His mother had intrauterine growth retardation and oligohydramnios at 32 weeks of gestational age. On his first physical examination, general remarkable findings, such as periumbilical collateral vessel formation, also referred to as caput medusa, were noted. He had developed fulminant liver failure with hypoproteinemia (total protein 3.2 g/dL, albumin 1.9 g/dL), hypoglycemia (29 mg/dL), jaundice, respiratory distress and hypotension during his first day of life. His serum aminotransferase levels were normal although a severe coagulopathy and hyperammonemia were present (Table 1). At 29 days of age, his serum hyaluronic acid concentration was elevated (2020 ng/mL). Thereafter, he died at 44 days of age due to multiorgan failure. Liver pathological findings at autopsy revealed the appearance of ductular metaplasia and pericellular fibrosis (Fig. 2).

Patient 2

The sister of patient 1 was born 1 year later at 30 weeks of gestational age by emergency cesarean section after severe intrauterine growth retardation, oligohydramnios and fetal distress were noted. Her birthweight was 822 g. She developed severe hypoglycemia

Journal compilation © 2008 Journal of Gastroenterology and Hepatology Foundation and Blackwell Publishing Asia Pty Ltd

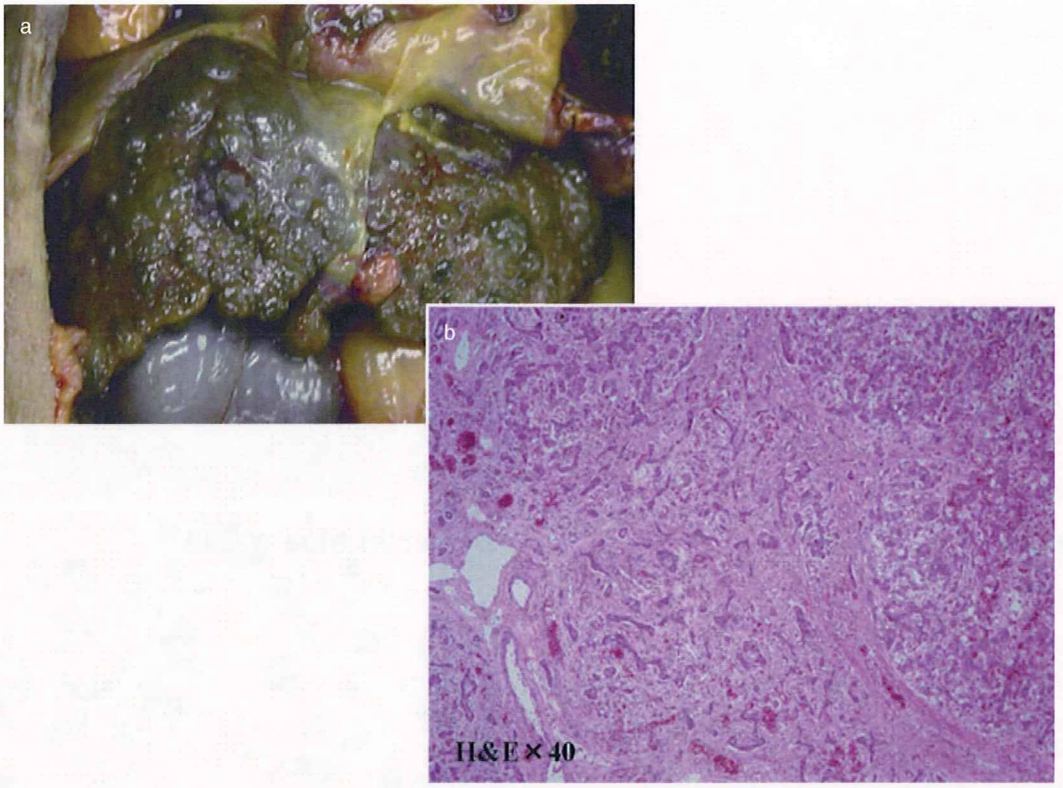

Figure 2 Liver pathological findings of patient 1. The liver was very atrophic and irregularly shaped on the surface at autopsy. Microscopically, the liver had extensive fibrosis, bile ductular proliferation of the surviving hepatocytes and extensive loss of hepatic parenchyma (hematoxylin and eosin staining; magnification ×40). The liver microscopic findings were very similar in patients 1 and 2.

(1 mg/dL), hypoproteinemia (total protein, 3.1 g/dL, albumin, 1.7 g/dL) and jaundice during her first day of life (her liver functional tests are listed in Table 1). On abdominal CT scan, ascites, an irregular liver edge and multiple low-density areas in the liver were observed. At 12 days of age, her hyaluronic acid concentration was elevated (4037 ng/mL). These findings suggested liver cirrhosis. This patient died as a result of liver and heart failure at 77 days of age. The liver pathological findings at autopsy were similar to those of patient 1.

Patient 3

A Japanese girl was born to a 36-year-old woman by spontaneous vaginal delivery without complication. Her birthweight was 3272 g. At 4 days of age, she was noticed to be deeply jaundiced (total bilirubin, 19.9 mg/dL); thereafter, she was admitted to Gunma Children's Medical Center due to liver dysfunction. Her admission laboratory studies are shown in Table 1. Her serum aminotransferase levels gradually decreased after admission; aspartate aminotransferase (AST) and alanine aminotransferase (ALT) fell to 22 U/L and 16 U/L, respectively at 10 days of age, but she developed acute liver failure. Liver magnetic resonance imaging (MRI) findings revealed a very low signal, especially on the T_2-weighted images. We suspected neonatal hemochromatosis based upon the laboratory data and consulted her parents regarding a living donor liver transplantation. However, her parents refused. Despite medical treatment, she died as a result of liver and respiratory failure at 32 days of age. The liver and pancreas macroscopic pathological findings at autopsy revealed cirrhotic severe atrophy and their color had changed to a brown, rust-like hue. The liver microscopic findings showed massive hepatic necrosis and the presence of hemosiderin granules in the metaplastic ductular epithelium (Fig. 3a,b). Positive hemosiderin granules were present diffusely in myocardial (Fig. 3c) and pancreas cells (Fig. 3d).

Patient 4

A full-term Japanese boy was born to a 20-year-old woman by cesarean section with cephalopelvic disproportion. His birthweight was 3814 g. At 14 days of age, he had vomiting, hepatosplenomegaly and liver dysfunction (Table 1). His serum aminotransferase levels gradually decreased after admission; the AST and ALT fell to 17 U/L and 13 U/L, respectively, at 17 days of age. He developed fulminant liver failure. The results of abdominal ultrasonography at 4 weeks of life revealed a small liver with patent portal and hepatic veins and mild ascites. The liver and pancreas MRI findings revealed a very low signal, especially on the T_2-weighted images. He died as a result of liver failure due to sepsis at 87 days of age. The liver microscopic findings at autopsy resembled those of patient 3.

Journal compilation © 2008 Journal of Gastroenterology and Hepatology Foundation and Blackwell Publishing Asia Pty Ltd

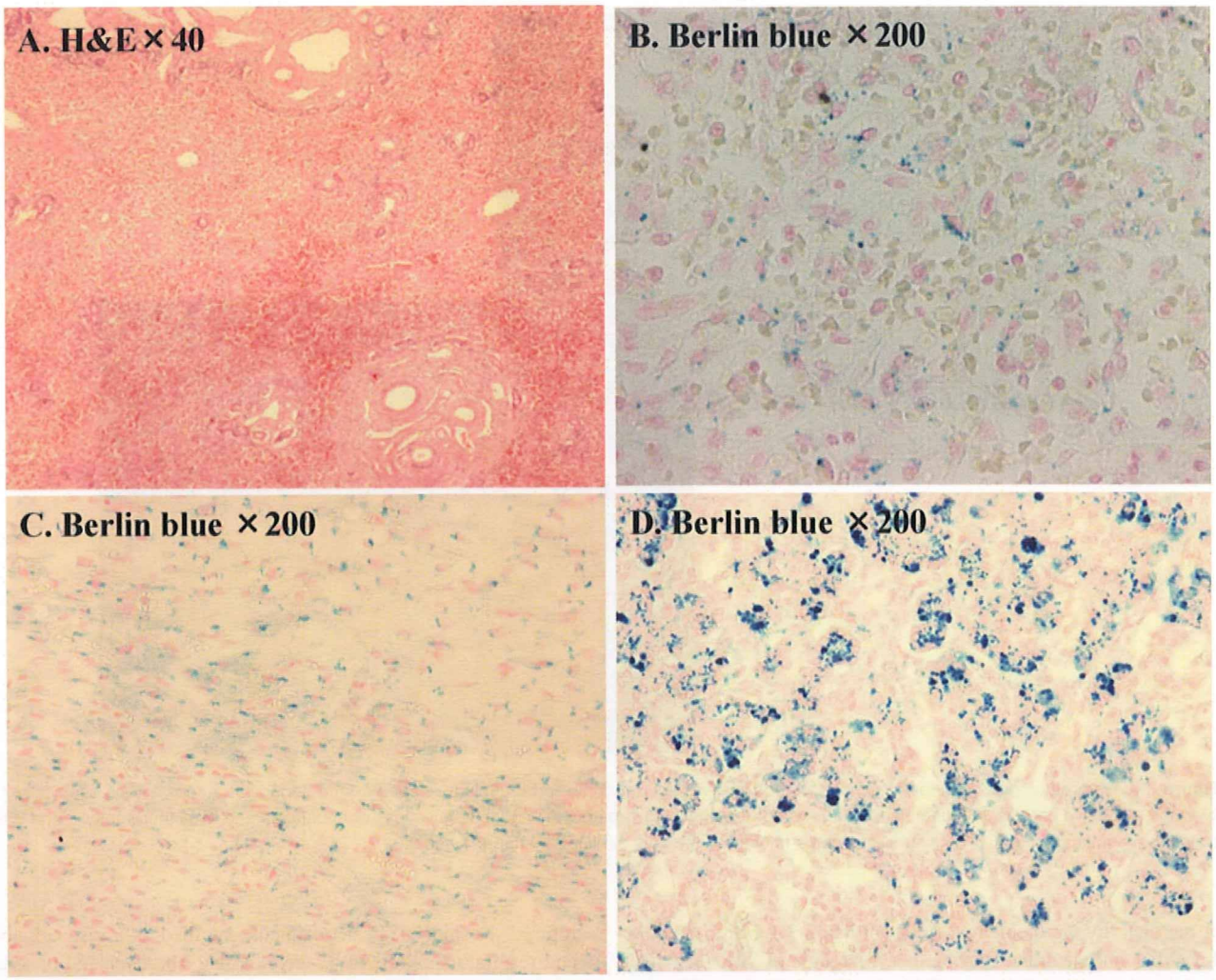

Figure 3 Liver pathological findings of patient 3. Microscopically, the liver specimen had extensive loss of hepatocytes with bile ductular proliferation and the portal areas approached one another (a, hematoxylin and eosin staining; magnification ×40). Hemosiderin was found predominantly in the metaplastic ductular epithelium (b, Berlin blue stain; magnification ×200). Positive hemosiderin granules are present diffusely in myocardial (c, Berlin blue stain; magnification ×200) and pancreas cells (d, Berlin blue stain; magnification ×200). The liver microscopic findings of patient 4 were similar to those of patient 3.

Patient 5

At 39 weeks of gestational age, a Japanese girl was born by spontaneous vaginal delivery without complication. Her birthweight was 2770 g. She was noticed to be jaundiced at 4 weeks of age; thereafter, her jaundice progressively worsened until 3 months of age. She became deeply icteric, with pale stools and dark urine. Her initial liver function tests on admission are shown in Table 1. Ursodeoxycholic acid (UDCA) (5 mg/kg per day) treatment was started immediately; thereafter, her serum bilirubin and aminotransferase levels gradually decreased (Fig. 4). However, we detected hyper-3-oxo-Δ^4 bile aciduria (Table 2). Accordingly, we recommended primary bile acid treatment for a suspected inborn error of bile acid synthesis. Her parents refused so we increased the dose of UDCA (to 10 mg/kg per day). At 11 months of age, her serum bilirubin and aminotransferase levels were within the normal range (Fig. 4). The serum concentration of the type IV collagen 7s domain also decreased to 4.0 ng/mL (normal range, <5.0 ng/mL) during UDCA treatment. However, we continued to detect hyper-3-oxo-Δ^4 bile aciduria after UDCA treatment. The liver biopsy microscopic findings at 8 months of age revealed giant cell transformation with bridging fibrosis and ductular proliferation (Fig. 5). We detected a heterozygous mutation in this patient (Fig. 6) by *SRD5B1* gene analysis and recommended *SRD5B1* gene analysis of the parents. However, her parents refused because she was in good health without liver dysfunction. At present, this patient remains in good health without any treatment.

Patient 6

A female Taiwanese infant with a birthweight of 3235 g was delivered at 38 weeks gestational age by spontaneous vaginal delivery

Journal compilation © 2008 Journal of Gastroenterology and Hepatology Foundation and Blackwell Publishing Asia Pty Ltd

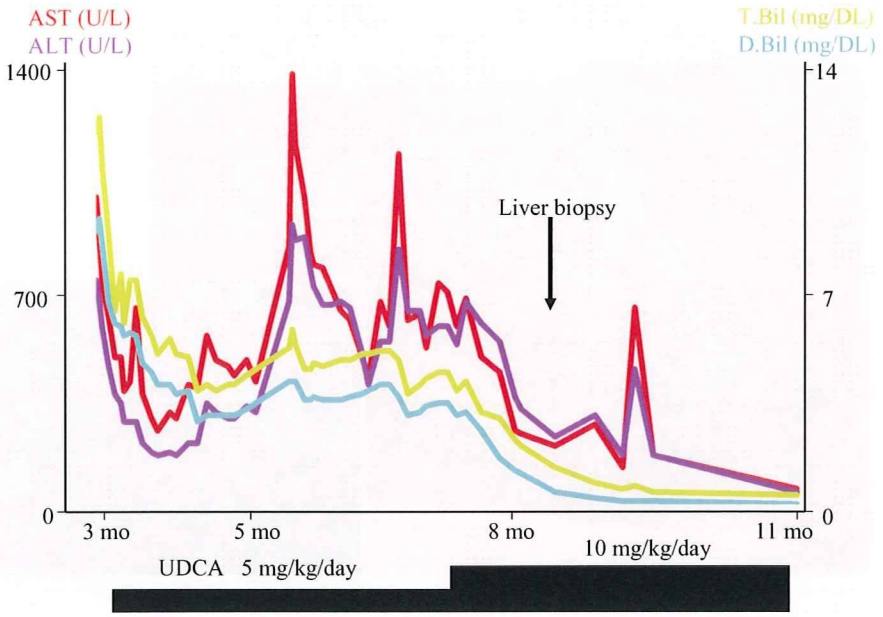

Figure 4 Clinical course of patient 5. Response of the serum bilirubin and aminotransferase levels to treatment with UCDA in patient 5. ALT, alanine aminotransferase; AST, aspartate aminotransferase; D.Bil, direct bilirubin; T.Bil, total bilirubin; UDCA, ursodeoxycholic acid.

Table 2 Bile acid analysis of the serum and urine using GC-MS in patients with hyper 3-oxo-Δ⁴ bile aciduria on admission

Patient		1	2	3	4	5-a	5-b	6-a	6-b	6-c
Serum	Cholic acid (%)	n.d.	n.d.		n.d.	n.d.	1.6	n.d.	n.d.	n.d.
	Chenodeoxycholic acid (%)	90.1	81.3		100.0	n.d.	7.1	17.5	99.2	79.1
	Ursodeoxycholic acid (%)	n.d.	n.d.		n.d.	34.3	n.d.	8.8	n.d.	20.9
	Allo-cholic acid (%)	n.d.	n.d.		n.d.	n.d.	27.0	n.d.	n.d.	n.d.
	Allo-chenodeoxycholic acid (%)	9.9	n.d.		n.d.	n.d.	17.9	n.d.	n.d.	n.d.
	CA-Δ⁴-3-one (%)	n.d.	n.d.		n.d.	27.2	17.6	n.d.	n.d.	n.d.
	CDCA-Δ⁴-3-one (%)	n.d.	n.d.		n.d.	38.4	6.8	73.7	n.d.	n.d.
	Others (%)	n.d.	18.7		n.d.	0.1	22.0	n.d.	0.8	n.d.
	Total bile acids (μmol/L)	30.3	0.5		8.4	8.5	9.8	9.2	54.9	6.1
Urine	Cholic acid (%)	4.4	5.5	n.d.	8.8	0.4	2.1	0.1	0.2	3.6
	Chenodeoxycholic acid (%)	2.4	n.d.	6.3	7.7	0.4	0.1	1.1	43.5	22.2
	Ursodeoxycholic acid (%)	0.1	2.9	0.4	n.d.	17.3	n.d.	8.2	0.2	24.7
	Allo-cholic acid (%)	n.d.	n.d.	n.d.	n.d.	n.d.	n.d.	n.d.	n.d.	n.d.
	Allo-chenodeoxycholic acid (%)	0.7	n.d.	14.7	2.5	n.d.	0.3	n.d.	n.d.	n.d.
	CA-Δ⁴-3-one (%)	5.1	48.3	n.d.	n.d.	64.7	87.6	51.0	18.8	7.6
	CDCA-Δ⁴-3-one (%)	86.2	40.9	63.3	73.1	14.3	6.5	35.8	27.7	15.8
	Others (%)	1.1	2.4	15.3	7.9	2.9	3.4	3.8	9.6	26.1
	Total bile acids (μmol/mmol Cr)	57.9	4.6	5.1	6.2	169.1	114.1	53.1	174.7	0.8

5-b, after the end of ursodeoxycholic acid (UDCA) treatment in patient 5 at 12 months of age; 6-a, before chenodeoxycholic acid treatment in patient 6 at 3 months of age; 6-b, 7 days after starting chenodeoxycholic acid treatment in patient 6 at 3 months of age; 6-c, mother of patient 6; we did not carry out a serum bile acid analysis in patient 3; CA-Δ⁴-3-one, 7α,12α-dihydroxy-3-oxo-4-cholenoic acid; CDCA-Δ⁴-3-one, 7α-hydroxy-3-oxo-4-cholenoic acid; n.d., not detected; 5-a, during UDCA treatment in patient 5 at 8 months of age.

after an uneventful pregnancy. At 2 months of age, the patient was referred to Taiwan University Hospital with a chief complaint of progressive jaundice (16.8 mg/dL). The stool color was light yellow. The jaundice present since birth was initially mild. Her initial physical examination on admission was nearly unremarkable without hepatosplenomegaly, jaundice or dark urine. Her liver functional tests at admission are shown in Table 1. Serial technetium-99*m* (^{99m}Tc)-DISIDA cholescintigraphy revealed visualization of intestinal radioactivity at 4.5 h postinjection. We started primary bile acid treatment with chenodeoxycholic acid (CDCA) (12 mg/kg per day) after analyzing her bile acids using GC-MS and her *SRD5B1* gene because we detected hyper 3-oxo-Δ⁴ bile aciduria (Table 2). A heterozygous mutation of the *SRD5B1* gene was found (Fig. 7). One month following the onset of CDCA administration, her total bilirubin and ALT levels decreased from 17.9 mg/dL and 342 U/L to 9.7 mg/dL and 235 U/L, respectively. CDCA treatment has continued until the present time. Her liver microscopic biopsy findings at 5 months of

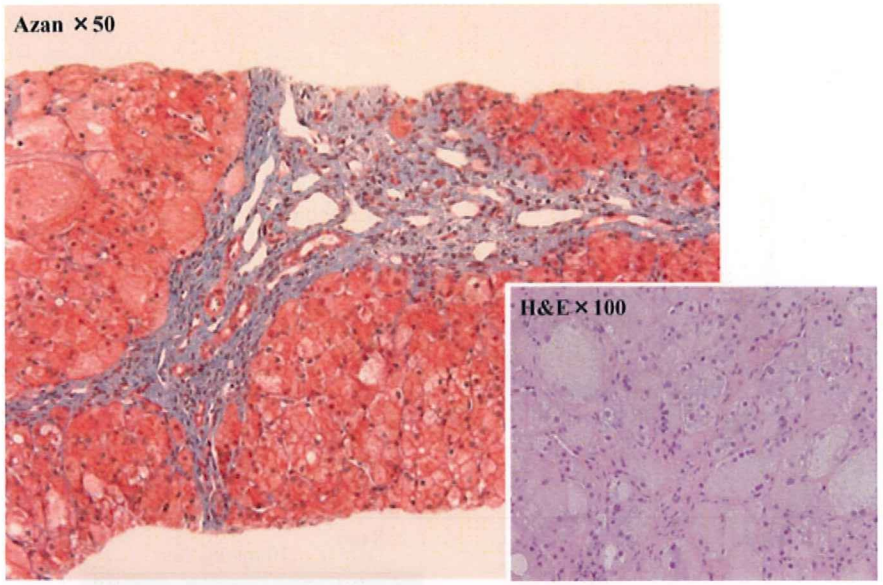

Figure 5 Liver pathological findings of patient 5. Liver biopsy specimen from patient 5 at 8 months shows lobular disarray resulting from extensive giant cell transformation (hematoxylin and eosin staining; magnification ×100) and consistent with cirrhosis showing wide fibrotic bands at the portal areas (Azan stain; magnification ×50). Bile ductular proliferation was noted. The liver microscopic findings of patient 6 were very similar to those of patient 5.

age revealed giant cell hepatitis with fibrosis similar to that of patient 5. Unfortunately, her liver function subsequently deteriorated and she was admitted to Taiwan University Hospital to be prepared for liver transplantation.

Patients 1–4 in the present study were treated with supportive care, such as blood exchange, administration of fresh frozen plasma, vitamin K and antibiotics. In all patients, the serum antibody titers showed no evidence of infection with hepatitis B or C virus, herpes simplex virus, Epstein–Barr virus or cytomegalovirus.

The parents of patients 1–6 were also in good health without liver dysfunction. However, in the mother of patient 6, we detected a high percentage of 3-oxo-Δ^4 bile acids relative to total bile acids (23.4%) in her urine (Table 2). Her liver functional tests were normal, including AST (17 U/L), ALT (7 U/L), total bilirubin (0.4 mg/dL) and GGT (7 U/L). Her GGT value was very low.

Qualitative and quantitative bile acid analysis

The serum and urine samples were collected and stored at −25°C until analysis. The concentrations of the individual bile acids in the urine were corrected for the creatinine (Cr) concentration and expressed as μmol/mmol of Cr.

After we synthesized some specific unusual bile acids, such as 3β-hydroxy-Δ^5,[11] 3-oxo-Δ^{412} and allo-bile acids,[13] as seen in inborn errors of bile acid synthesis, we routinely analyzed the bile acids in the urine and serum by GC-MS using selected ion monitoring of the characteristic fragments of the methyl ester-dimethylethylsilyl ether-methoxime derivatives of the bile acids as described previously,[14] after enzymatic hydrolysis (choloylglycine hydrolase 30 units) and solvolysis (sulfatase 150 units; Sigma Chemical Co., St Louis, MO, USA).

All the patients in this study had the bile acids in their serum and urine analyzed using GC-MS on admission.

Genetic analysis

With informed consent, liver tissue (patients 1 and 2), blood (patients 3, 5 and 6) and nails (patient 4) were collected from the patients and parents of patient 6, as well as 103 healthy Asian individuals. The genomic DNA was extracted from liver tissues, peripheral leukocytes and nails using a QIAamp Mini Kit (Qiagen, Hilden, Germany).

The DNA fragments spanning the nine coding regions of the *SRD5B1* genes were amplified by polymerase chain reaction (PCR) using Gene Taq (Nippon Gene, Toyama, Japan) and nine sets of primers (F1: 5′-CTTTCTTTGATGGAATAGGC-3′ and B1: 5′-AGTAAGTCAATGAGATCTGC-3′, F2: 5′-TGTACATGCAA AATGTCCTG-3′ and B2: 5′-ATGAGTGCAATTACACACAC-3′, F3: 5′-TTACAAAGAAAAAGGGGCTG-3′ and B3: 5′-CTTC ATGCACATAGCTATTG-3′, F4: 5′-GCTCACAATTATGAAGA CTG-3′ and B4: 5′-TCATTGAAAGTAAAGGGTGC-3′, F5: 5′-TGCTTATTAACATACCCAGG-3′ and B5: 5′-ATTTAGGTGG AGCAATCATG-3′, F6: 5′-AATTGCATTCAACAACGTGG-3′ and B6: 5′-AACCAAAAGGCATTCCAATC-3′, F7: 5′-GAGG AGGATGGTTTATTAAC-3′ and B7: 5′-GGTTTCCTATTAAG CTGAAC-3′, F8: 5′-TTCATACATCTTTGGAAGGC-3′ and B8: 5′-TCAGGCATGTTAACATTCAG-3′, F9: 5′-AACAGCAGAGG AATGAATAG-3′ and B9: 5′-AACCCTCTCTCTTCATTTTC-3′) to obtain the optimal length of DNA fragments suitable for direct sequence analysis.[15] The temperature program included an initial denaturation step of 94°C for 2 min followed by 30 cycles of a denaturation step of 94°C for 1 min, annealing at 59°C for 1 min, and extension at 72°C for 1 min. A final extension step of 72°C for 10 min was used using a T3 thermocycler (Whatman, Kent UK).

After enzyme processing with ExoSAP-IT (USB Co., Cleveland, OH, USA), direct sequencing of the amplified PCR products was carried out with the DTCS Quick Start Kit (Beckman Coulter, Fullerton, CA, USA) according to the manufacturer's protocol,

Journal compilation © 2008 Journal of Gastroenterology and Hepatology Foundation and Blackwell Publishing Asia Pty Ltd

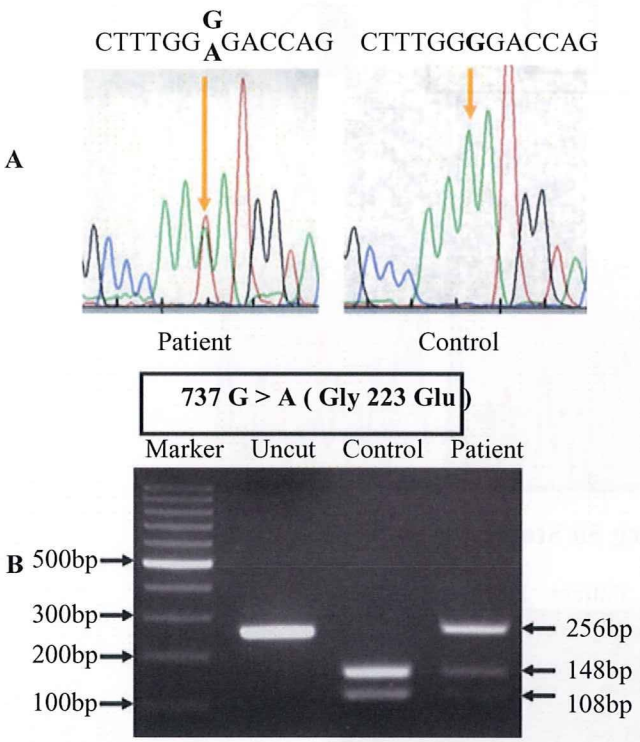

Figure 6 DNA analysis in patient 5 and a healthy control. (a) Genomic DNA sequence of the 3-oxo-Δ^4-steroid 5β-reductase gene. The position of the nucleotide sequence in the mutation is shown with arrows. The arrow identifies G/A in the patient and G in a control subject. The reverse-strand sequence showed the same result. This represents a CGA-to-TGA mutation, affecting glycine at position 223, where it is replaced by glutamate. Such a nucleotide substitution was not observed in the 103 controls (the wild-type nucleotide 'G' is seen in the control example). (b) Digestion of amplified SDR5B1 exon 6 polymerase chain reaction (PCR) fragment with *Ava*II. To screen for the novel G-to-A mutation at nucleotide 737, we amplified the PCR products of *SRD5B1* gene exon 6. The PCR products from the healthy control allele were digested by the *Ava*II enzyme (at G/GWCC, W. A or T) into two fragments, whereas the mutant form of the allele was not digested. The patient was confirmed to be heterozygous for G-to-A substitution, as he showed digested and non-digested fragments.

using the same primers as for PCR amplification. The sequencing reaction product was analyzed electrophoretically, using a SEQ2000XL analyzer (Beckman Coulter).

Once the two putative mutations were found, six patients, the parents of patient 6 and 103 healthy Asian individuals were screened for these two mutations by digesting the appropriate PCR fragment with a restriction enzyme. *Ava*II (Takara, Shiga, Japan) was used to recognize the G/GW (A or T) CC sequence in the exon 6 PCR fragment for the mutation found in patient 6, while *Kpn*I (Takara, Shiga, Japan) was used to recognize the GGTAC/C sequence in the exon 2 PCR fragment for the mutation found in patient 5. The restricted DNA fragments were separated by electrophoresis on a 1.5% agarose gel and then stained with ethidium bromide.

Results

Patient profile and liver pathology

Patient profile and liver pathology are shown in Table 1 and Figures 2, 3 and 5. Four patients, patients 1–4, developed neonatal liver failure, while the other patients, patients 5 and 6, showed chronic cholestasis. Patients 1 and 2 immediately developed fulminant liver failure after emergency cesarean sections due to fetal distress at late gestational age. Moreover, these patients had complications evident during pregnancy, such as intrauterine growth retardation and oligohydramnios, and did not have an elevated AST or ALT after birth. Patients 3 and 4 developed liver failure 1 or 2 weeks after delivery, respectively, with elevated ferritin concentrations. All patients had severe jaundice and abnormal prothrombin times except for one patient. The total bile acid and GGT values were low in all but two patients, patients 1 and 2 and patients 2 and 5, respectively. In addition, the liver pathological findings of the patients are shown in Figures 2, 3 and 5.

Biochemical identification of an inborn error of bile acid synthesis

Biochemical identification of an inborn error of bile acid synthesis is shown in Table 2. In the serum, the main bile acid in the patients with liver failure, patients 1, 2 and 4, was CDCA. We detected large amounts of 3-oxo-Δ^4 bile acids in the serum of patients with chronic cholestasis, patients 5 and 6, prior to treatment. Patient 5 had a decreased percentage of 3-oxo-Δ^4 bile acids relative to the total bile acids in the serum after the end of the UDCA treatment. We did not detect 3-oxo-Δ^4 bile acids in the serum of patient 6 during the CDCA treatment.

We detected large amounts of 3-oxo-Δ^4 bile acids in the urine of all the patients. In the patients with liver failure, the main 3-oxo-Δ^4 bile acid in the urine was 7α-hydroxy-3-oxo-4-cholenoic acid. Patients 5 and 6 had increased excretion of urinary bile acids during bile acid treatment compared to that without treatment, and a decreased percentage of 3-oxo-Δ^4 bile acids relative to the urinary total bile acids during the bile acid treatment.

We detected urinary 3-oxo-Δ^4 bile acids in the mother of patient 6; however, we could not detect 3-oxo-Δ^4 bile acids in the serum or urine in the father of patient 6.

Identification of SDR5B1 gene defects

We did not detect a mutation in the *SRD5B1* gene of patients 1–4. We have identified two single-nucleotide changes in two patients. A single substitution of G to A at nucleotide position 737 was confirmed in exon 6 of the *SRD5B1* gene, which causes an amino acid change from glycine (GGG) to glutamate (GAG) at amino acid position 223 in patient 5. This novel mutation was identified as a heterozygous mutation (Fig. 6).

In patient 6, a single substitution of C to T at nucleotide position 217 was confirmed in exon 2 of the SDR5B1 gene, which causes an amino acid change from arginine (CGA) to stop (TGA) at amino acid position 50. This novel mutation was identified as a heterozygous mutation in the patient and her mother (Fig. 7).

Journal compilation © 2008 Journal of Gastroenterology and Hepatology Foundation and Blackwell Publishing Asia Pty Ltd

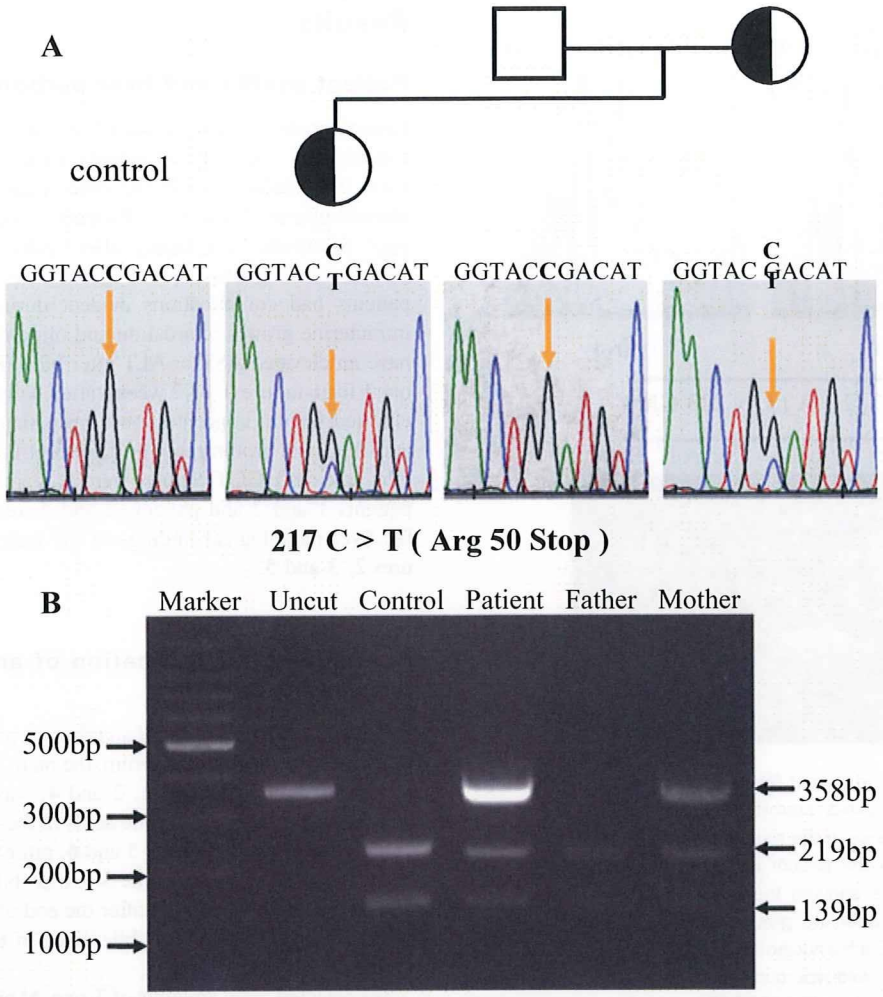

Figure 7 DNA studies of patient 6, her parents and a control. (a) Pedigree and DNA sequence of the 3-oxo-Δ⁴-steroid 5β-reductase gene in genomic DNA samples. The position of the mutant nucleotide sequence is shown with arrows, indicating C/T in the patient and her mother, and C in her father and a control subject. The reverse strand sequence showed the same result. This represents a CGA-to-TGA mutation, affecting arginine at position 50, which is replaced by a stop codon. Such a nucleotide substitution was not observed in the 103 controls (the wild-type nucleotide 'C' appears in the selected control). (b) Digestion of amplified SRD5B1 exon 2 PCR fragment with *Kpn*I. To screen for the novel C-to-T mutation at nucleotide 217, we amplified the PCR products of *SRD5B1* gene exon 2. The PCR products from the patient's father and a control example were digested by the *Kpn*I enzyme (GGTAC/C) into two fragments. The patient and her mother showed both digested and non-digested fragments, with the latter representing the mutation; this indicates that they were heterozygous for the mutation.

Neither of these mutations was found in 103 healthy Asian individuals.

Discussion

We identified two patients with heterozygous mutations of primary 3-oxo-Δ⁴-steroid 5β-reductase deficiency by *SRD5B1* gene analysis. According to previous reports[7,8] of the mutations in the *SRD5B1* gene of the five reported patients, three were homozygous and two were compound heterozygous. Furthermore, this enzyme deficiency was reported as displaying an autosomal recessive transmission pattern. Although our two patients appear to have an autosomal recessive transmission pattern, we suspect that the father of patient 6 may have a heterozygous mutation outside the coding region, such as in the promoter region or in an intron. We do not know about patient 5 because we could not carry out *SRD5B1* gene analysis in the parents of patient 5. However, we suspect that one of the parents of patient 5 may have heterozygous mutations outside the coding region. Therefore, we suggest that our two patients with chronic cholestasis may be compound heterozygotes of the *SRD5B1* gene.

Although both patients 5 and 6 have a heterozygous mutation in the *SRD5B1* gene, these patients may have cholestasis with liver dysfunction only during infancy; patient 5 actually had a favorable course without bile acid replacement therapy. Thereafter, the cholestasis with liver dysfunction in this disease may gradually

improve, as the mother of patient 6 does not have liver dysfunction. Because neonatal bile acid metabolism is different from that of adults, 3-oxo-Δ^4-steroid 5β-reductase may be essential during the newborn period. In healthy full-term infants, we detect a high percentage of urinary 3-oxo-Δ^4 bile acids in the total bile acids during the early neonatal period. This reflects the normal development of bile acid metabolism, including the initial immaturity of 3-oxo-Δ^4-steroid 5β-reductase.[14,16] In the newborn period, patients with a heterozygous mutation in the *SRD5B1* gene may develop cholestasis with liver dysfunction that can resolve later. However, the same patient may develop a severe stage of disease similar to that of patient 6.

Moreover, we would still suspect that patients with a heterozygous mutation of the *SRD5B1* gene may have mutations in another gene. We have completed coding region analysis of the bile salt export pump gene (BSEP) in patient 6. However, we could not find mutations in BSEP, except for a heterozygous Val 444 Ala polymorphism.

In this study, a primary 3-oxo-Δ^4-steroid 5β-reductase deficiency could not be diagnosed solely by low or normal levels of GGT activity and the total bile acid concentration by an enzymatic technique using 3α-hydroxysteroid dehydrogenase, or the presence of hyper 3-oxo-Δ^4 bile aciduria. Patients with fulminant hepatic failure, patients 1–4, did not have detectable 3-oxo-Δ^4 bile acids in their serum, whereas it was detected in the serum of patients 5 and 6. This may be a very important observation. Lemonds and Clayton also suggested that the detection of 3-oxo-Δ^4 bile acids and trace amounts of CDCA in the serum are important findings in the differential diagnosis.[7] However, Sumazaki had reported a patient with an extremely reduced activity of 3-oxo-Δ^4-steroid 5β-reductase without any genetically defined defects and who had large amounts of 3-oxo-Δ^4 bile acids in the serum and urine.[17] Therefore, we suggest that the pediatric physician must analyze the bile acids in the serum and urine using GC-MS when one suspects a primary 3-oxo-Δ^4-steroid 5β-reductase deficiency based upon the values of the GGT activity and the total bile acid concentration. If high concentrations of 3-oxo-Δ^4 bile acids are detected in the serum and urine, one should analyze the *SRD5B1* gene.[7]

In our patient 5, the liver function tests, including type IV collagen 7s domain, gradually improved with UDCA treatment (Fig. 4). However, we detected 3-oxo-Δ^4 bile acids in the serum and urine after UDCA treatment (or when not on any current treatment) (Table 2).

Of the patients with fulminant hepatic failure, patients 1–4 were diagnosed as having neonatal hemochromatosis by their clinical symptoms, such as intrauterine growth retardation, oligohydramnios, fetal distress and hypoglycemia, their laboratory data, such as elevated ferritin concentration, the liver pathological findings, and the results of *SRD5B1* gene analysis. We suggest that patients 1 and 2 had fetal hemochromatosis whereas patients 3 and 4 were diagnosed as having infantile (neonatal) hemochromatosis.[18,19] The reason for the reduced activity of hepatic 3-oxo-Δ^4-steroid 5β-reductase was a partial enzyme deficiency predisposing to severe hepatocyte damage.[16] Therefore, we suggest that these patients did not have a primary defect in the *SRD5B1* gene. We believe that pediatric hepatologists should not stop searching for a cause of any hepatocyte damage after the discovery of hyper 3-oxo-Δ^4 bile aciduria with neonatal liver failure;[20] that is, pediatric hepatologists should carry out *SRD5B1* gene analysis to distinguish between a primary 3-oxo-Δ^4-steroid 5β-reductase deficiency from a secondary defect in the presence of hyper-3-oxo-Δ^4 bile aciduria. Our experience indicates that until a specific diagnostic test is devised, *SRD5B1* gene analysis will remain essential for research and for accurate diagnosis of primary 3-oxo-Δ^4-steroid 5β-reductase deficiency, especially when the deficiency occurs sporadically.

In conclusion, we suggest that patients with fulminant hepatic failure who have hyper-3-oxo-Δ^4 bile aciduria during the neonatal period may have secondary 3-oxo-Δ^4-steroid 5β-reductase deficiency based upon our results of *SRD5B1* gene analysis. However, patients with chronic cholestasis who have hyper-3-oxo-Δ^4 bile aciduria are more likely to have primary 3-oxo-Δ^4-steroid 5β-reductase deficiency based upon the detected heterozygous mutations in the *SRD5B1* gene. Therefore, SDR5B1 gene analysis is necessary for the accurate diagnosis of 3-oxo-Δ^4-steroid 5β-reductase deficiency. Moreover, from the results of the *SRD5B1* gene analysis, we think that it is important to elucidate whether there is a heterozygous or compound heterozygous mutation in our two patients.

References

1 Shneider BL, Setchell KDR, Whitington PF, Neilson KA, Suchy FJ. Δ^4-3-Oxosteroid 5β-reductase deficiency causing neonatal liver failure and hemochromatosis. *J. Pediatr.* 1994; **124**: 234–8.

2 Siafakas CG, Jonas MM, Perez-Atayde AR. Abnormal bile acid metabolism and neonatal hemochromatosis: a subset with poor prognosis. *J. Pediatr. Gastroenterol. Nutr.* 1997; **25**: 321–6.

3 Kimura A, Suzuki M, Murai T *et al.* Urinary 7α-hydroxy-3-oxochol-4-en-24-oic and 3-oxochola-4,6-dien-24-oic acids in infants with cholestasis. *J. Hepatol.* 1998; **28**: 270–9.

4 Kimura A, Suzuki M, Tohma M *et al.* Increased urinary excretion of 3-oxo-Δ^4 bile acids in Japanese patients with idiopathic neonatal cholestasis. *J. Pediatr. Gastroenterol. Nutr.* 1998; **27**: 606–9.

5 Setchell KDR, Suchy FJ, Welsh MB, Zimmer-Nechemias L, Heubi J, Balistreri WF. Δ^4-3-Oxosteroid 5β-reductase deficiency described in identical twins with neonatal hepatitis. *J. Clin. Invest.* 1988; **82**: 2148–57.

6 Kondo K-H, Kai M-H, Setoguchi Y *et al.* Cloning and expression of cDNA of human Δ^4-3-oxosteroid 5β-reductase and substrate specificity of the expressed enzyme. *Eur. J. Biochem.* 1994; **219**: 357–63.

7 Lemonde HA, Custard EJ, Bouquet J *et al.* Mutations in SRD5B1 (AKR1D1), the gene encoding Δ^4-3-oxosteroid 5β-reductase, in hepatitis and liver failure in infancy. *Gut* 2003; **52**: 1494–9.

8 Gonzales E, Cresteil D, Baussan C, Dabadie A, Gerhardt M-F, Jacquemin E. SRD5B1 (AKR1D1) gene analysis in Δ^4-3-oxosteroid 5β-reductase deficiency: evidence for primary genetic defect [letter]. *J. Hepatol.* 2004; **40**: 716–18.

9 Daugherty C, Setchell KDR, Heubi J, Balistreri WF. Resolution of liver biopsy alterations in three siblings with bile acid treatment of an inborn error of bile acid metabolism (Δ^4-3-Oxosteroid 5β-reductase deficiency). *Hepatology* 1993; **18**: 1096–101.

10 Clayton PT, Molls KA, Johnson AW, Barabino A, Marazzi MG. Δ^4-3-Oxosteroid 5β-reductase deficiency: failure of ursodeoxycholic acid treatment and response to chenodeoxycholic acid plus cholic acid. *Gut* 1996; **38**: 623–8.

Journal compilation © 2008 Journal of Gastroenterology and Hepatology Foundation and Blackwell Publishing Asia Pty Ltd

11 Tohma M, Mahara R, Takeshita H, Kurosawa T. A convenient synthesis of 3β,12α-, 3β,7α-, and 3β,7β-dihydroxy-5-cholen-24-oic acids: unusual bile acids in human biological fluids. *Steroid* 1986; **48**: 331–8.
12 Leppik RA. Improved synthesis of 3-keto, 4-ene-3keto-, and 4,6-diene-3-keto bile acids. *Steroid* 1983; **41**: 475–84.
13 Iida T, Nishida S, Chang FC, Niwa T, Goto J, Nambara T. Potential bile acid metabolism. XXI. A new synthesis of allochenodeoxycholic and allocholic acids. *Chem. Pharm. Bull.* 1993; **41**: 763–5.
14 Kimura A, Mahara R, Inoue T *et al.* Profile of urinary bile acids in infants and children: developmental pattern of excretion of unsaturated ketonic bile acids and 7β-hydroxylated bile acids. *Pediatr. Res.* 1999; **45**: 603–9.
15 Charbouneau A, Luu The V. Genomic organization of a human 5β-reductase and its pseudogene and substrate selectivity of the expressed enzyme. *Biochem. Biophys. Acta* 2001; **1517**: 228–35.
16 Inoue T, Kimura A, Aoki K, Tohma M, Kato H. Developmental pattern of 3-oxo-Δ^4 bile acids in neonatal bile acid metabolism. *Arch. Dis. Child* 1997; **77**: F52–6.
17 Sumazaki R, Nakamura N, Shoda J, Kurosawa T, Tohma M. Gene analysis in Δ^4-3-oxosteroid 5β-reductase deficiency. *Lancet* 1997; **349**: 329.
18 Whitington PF, Kelly S, Ekong UD. Neonatal hemochromatosis: fetal liver disease leading to liver failure in the fetus and newborn. *Pediatr. Transplant.* 2005; **9**: 640–5.
19 Whitington PF. Fetal and infantile hemochromatosis. *Hepatology* 2006; **43**: 654–60.
20 Clayton PT. Δ^4-3-oxosteroid 5β-reductase deficiency and neonatal hemochromatosis [letter]. *J. Pediatr.* 1994; **125**: 845–6.

Clinica Chimica Acta 406 (2009) 52–56

Contents lists available at ScienceDirect

Clinica Chimica Acta

journal homepage: www.elsevier.com/locate/clinchim

Lipoprotein profiles in children with two common cholesteryl ester transfer protein gene mutations, D442G and I14A, during the first year of life

Hironori Nagasaka [a,*], Tohru Yorifuji [b], Toru Momoi [b], Junko Yorifuji [b], Kenichi Hirano [c], Akemi Ota [c], Tomozumi Takatani [a], Hirokazu Tsukahara [d], Masaki Takayanagi [a], Kunihiko Kobayashi [f], Hitoshi Chiba [e], Yukiyasu Sato [g], Takashi Miida [h]

[a] Division of Metabolism, Chiba Children's Hospital, Chiba 266-0007, Japan
[b] Department of Pediatrics, Kyoto University, Graduate School of Medicine, Kyoto 606-8507, Japan
[c] Department of Cardiovascular Medicine, Osaka University, Graduate School of Medicine, 565-0871, Japan
[d] Department of Pediatrics, Fukui University, Graduate School of Medicine, Fukui 910-1193, Japan
[e] Department of Health Science, Hokkaido University School of Medicine, Sapporo 060-8638, Japan
[f] Department of Pediatrics, Hokkaido University, Graduate School of Medicine, Sapporo 060-8638, Japan
[g] Department of Gynecology & Obstetrics, Kyoto University, Graduate School of Medicine, Kyoto 606-8507, Japan
[h] Department of Clinical Laboratory Medicine, Juntendo University School of Medicine, Tokyo 113-8421, Japan

ARTICLE INFO

Article history:
Received 29 January 2009
Received in revised form 11 May 2009
Accepted 12 May 2009
Available online 19 May 2009

Keywords:
CETP
D442G and I14A
Early life
ApoE-rich HDL
LDL

ABSTRACT

Background: Hyperalphalipoproteinemia is associated with cholesteryl ester transfer protein (CETP) deficiency in adults but has unclear associations in children.
Methods: We measured lipoproteins in 19 heterozygotes (D442G, $n=17$; I14A, $n=2$), one D442G/I14A compound heterozygote, 13 non-affected siblings, and 30 healthy controls at birth, 3–4 months, and 12 months.
Results: CETP mass was 32–70% lower in heterozygotes than in controls throughout the year. Low-density lipoprotein-cholesterol (LDL-C) was lower in heterozygotes than in controls by 30, 20, and 15% at birth, 3–4 months, and 12 months, respectively. High-density lipoprotein-cholesterol (HDL-C) was similar among the groups at birth, but was 10% higher in heterozygotes compared with controls at 3–4 and 12 months. ApoE-rich HDL-C was similar between the two groups at birth, but was 50% higher in heterozygotes than in controls at 3–4 and 12 months. These lipoprotein profile characteristics were prominent in the compound heterozygote but were not found in non-affected siblings. In heterozygotes, CETP mass correlated positively with LDL-C but negatively with HDL-C at 3–4 and 12 months.
Conclusion: CETP is a determinant for LDL-C and HDL-C in CETP-deficient individuals in the first year of life.
© 2009 Elsevier B.V. All rights reserved.

1. Introduction

Lipoprotein metabolism in young children changes during growth and development [1–5]. At birth, high-density lipoprotein (HDL) accounts for the majority of plasma lipoprotein particles, and plasma concentrations of low-density lipoprotein (LDL) are quite low. After the initial feeding, plasma LDL increases rapidly, and HDL changes both qualitatively and quantitatively.

Cholesteryl ester transfer protein (CETP) promotes cholesteryl ester (CE) transfer from HDL to very low-density lipoprotein (VLDL) and LDL [6–9]. CETP exhibits the highest activity early in life and, in particular, at birth [1,5]. Recently, we studied lipoprotein profiles in children without and with familial hypercholesterolemia (FH), during the first year of life. At birth, apolipoprotein E (ApoE)-rich HDL (a better substrate for CETP than apoE-poor HDL) concentrations were much lower in individuals with FH than in controls, although CETP mass concentrations were similar between the groups. The mean LDL concentration in controls was only 25 mg/dl, which is approximately half the level measured in individuals with FH, suggesting that low acceptor lipoprotein (LDL) concentrations may restrict cholesterol ester (CE) transfer from HDL to a greater extent than CETP mass [5].

Two common mutations occur in the CETP gene—an intron 14 splicing donor site mutation (I14A) and a missense mutation in exon 15 (D442G). Adults with these mutations exhibit high HDL-cholesterol (HDL-C) levels [6–9]. As the levels of acceptor lipoproteins for CE are very low in early life, CETP may not be important for CE transfer in newborn babies with CETP deficiency. To examine whether CETP is a determinant for LDL-C and HDL-C in the first year of life, we serially

Abbreviations: CETP, cholesteryl ester transfer protein; CE, cholesteryl ester; ApoE, apolipoprotein E; FH, familial hypercholesterolemia; I14A, an intron 14 splicing donor site mutation in the CETP gene; D442G, a missense mutation in exon 15 in the CETP gene; PEG, polyethylene glycol; DS-PT-Mg, dextran sulfate-sodium phosphotungstate-MgCl1.

* Corresponding author. Chiba Children's Hospital, 579-1 Heta Cho, Midori-Ku, Chiba, Japan. Tel.: +81 43 292 2111; fax: +81 43 292 3815.
E-mail address: nagasa-hirono@k2.dion.ne.jp (H. Nagasaka).

0009-8981/$ – see front matter © 2009 Elsevier B.V. All rights reserved.
doi:10.1016/j.cca.2009.05.007

determined LDL-C and HDL-C concentrations as well as other parameters in children without and with CETP gene mutations.

2. Methods

2.1. Subjects

We examined 370 newborns with normal birth weights for CETP mutations. Among these, 17 heterozygotes for the D442G mutation (9 boys and 8 girls), 2 heterozygotes for the Int14A mutation (2 girls), and 1 compound heterozygote for D442G/I14A (a boy) were found (Table 1). Furthermore, 10 heterozygotes (5 boys and 5 girls) with the D442G mutation were born from 8 mothers with this mutation. Of the 2 heterozygotes for the Int14A mutation, 1 was born from a mother with the same mutation. The mother and father of the compound heterozygote were heterozygotes for I14A and D442G, respectively.

We examined the lipoprotein profiles in these children and compared them with the profiles measured in their 13 non-affected siblings (7 boys and 6 girls) and in 30 healthy children (15 boys and 15 girls) with normal birth weights (Table 1). Of the 13 non-affected siblings, seven (3 boys and 4 girls) were born from 6 mothers with the D442G mutation and one mother with the I14A mutation.

All subjects were fed mother's milk during the first 2 months and artificial milk thereafter. They were all healthy, with the exception of upper respiratory infections contracted during the first year of life. The protocol was approved by the ethics committees of the participating institutions, and written informed consent was obtained from the parents of all subjects.

2.2. Determinations of lipid, apolipoprotein, and CETP mass levels

Fasting serum samples were obtained from cord veins at birth and from cubitus veins at 3–4 and 12 months. All procedures for lipid and apolipoprotein (apo) measurements were completed within 1 day using fresh samples. Total cholesterol (TC) and triglyceride (TG) concentrations were measured enzymatically. We quantified HDL fractions using 2 precipitating reagents: 13% polyethylene glycol (PEG; PEG 6000, Wako Pure Chemicals, Osaka, Japan) and dextran sulfate-sodium phosphotungstate-MgCl2 (DS-PT-Mg; HDL-C Daiichi, Daiichi Pure Chemicals) [1,5,6]. PEG precipitates apoB-containing lipoproteins but not HDL composed of apoE-poor HDL and apoE-rich HDL, whereas DS-PT-Mg precipitates apoE-rich HDL together with apoB-containing lipoproteins. Accordingly, total HDL-C and apoE-poor HDL-C concentrations were defined as the cholesterol concentrations in the supernatants after precipitation with PEG and DS-PT-Mg, respectively. The apoE-rich HDL concentration was calculated by subtracting the apoE-poor HDL-C concentration from total HDL-C. This method was validated using serum obtained from CETP-deficient subjects and newborns, by lipid staining following agarose-gel electrophoresis, chromatography, and/or immunofixation [1,6,10]. LDL-C concentrations were determined by a homogeneous assay (Cholestest LDL-C, Daiichi Pure Chemicals, Tokyo, Japan). Apo A-I, A-II, B, and E levels were measured by turbidimetric immunoassays (Daiichi Pure Chemicals). CETP mass was measured by sandwich enzyme immunoassay using frozen samples [11].

2.3. Analyses of the D442G and Int14A mutations

Genomic DNA was prepared using a commercial kit (SMJ TEST, Sumitomo Kinzoku, Kanagawa, Japan). Polymerase chain reaction (PCR) was performed using the following nucleotide primers: F-D442G, 5′-ACACCCCTCATCAACACCAAAGGCGTGAGCCTCTCCG-3′; R-D442G, 5′-AAGGGAGGGGCAGTAGGAGA-3′; F-I14A, 5′-CACGGATGGGCATGAGGATG-3′; and R-I14A, 5′-AAGCTCTGTCAGCCTCGGCACCCAGTTTCCCCGCCAGCCCACACATA-3′. F-D442G and R-I14A were modified to generate MspI and NdeI endonuclease cleavage sites [8].

2.4. Statistical analyses

Statistical differences in lipoprotein profiles between children with and without CETP mutations were estimated. Similarly, the relationships between CETP mass and lipid levels were statistically estimated in the heterozygous children and controls. All pairwise comparisons were performed using a 2-sided Student's *t*-test. The correlation analyses were examined by Pearson's correlation test. Values of $p<0.05$ were considered significant.

3. Results

3.1. The incidences of D442G and I14A

The incidences of D442G and I14A were 4.9% and 0.81%, respectively, which is nearly consistent with the prevalence of these mutations in the Japanese population [7–9,12].

Table 1
Changes in serum lipid, apolipoprotein, and CETP concentrations during the first year of life.

	Compound heterozygote ($n=1$)	Heterozygotes for I14A ($n=2$)	Heterozygotes for D442G ($n=17$)	Non-affected siblings ($n=13$)	Age-matched healthy controls ($n=30$)
M/F	1/0	0/2	9/8	7/6	15/15
Gest. P (weeks)	38	39, 41	38–41	36–41	38–41
Birth weight (g)	2775	2881–3101	2726–3302	2616–3444	2689–3465
CETP (mg/l)					
At birth	0.5	1.2/1.6	1.9 (0.5)[c]	3.2 (1.3)	2.8 (1.2)
3–4 M	0.3	0.8/0.9	1.7 (0.5)[c]	2.5 (0.6)	2.6 (0.6)
12 M	0.3	1.0/1.2	1.6 (0.5)[c]	2.5 (0.8)	2.6 (1.1)
TC					
At birth	48	51/52	57 (8)[a]	64 (16)	64 (7)
3–4 M	123	109/127	133 (13)[a]	153 (21)	151 (19)
12 M	128	121/127	141 (11)[a]	156 (24)	153 (22)
TG					
At birth	23	25/15	23 (5)	27 (13)	21 (7)
3–4 M	49	70/86	82 (12)	90 (27)	88 (31)
12 M	58	76/60	85 (11)	88 (30)	80 (25)
LDL-C					
At birth	6	13/13	17 (5)[b]	25 (7)	24 (6)
3–4 M	30	42/52	56 (10)[b]	75 (15)	72 (13)
12 M	36	59/65	65 (12)a	78 (19)	75 (16)
Total HDL-C					
At birth	37	32/36	36 (5)	36 (12)	34 (9)
3–4 M	84	57/60	61 (5)[a]	55 (11)	54 (8)
12 M	87	59/65	62 (7)[a]	56 (12)	54(10)
ApoE(+)HDL-C					
At birth	14	9/11	11 (4)	11 (4)	11 (4)
3–4 M	24	16/16	13 (3)[b]	8 (1)	9 (3)
12 M	29	10/12	11 (2)[a]	7 (1)	7 (2)
ApoE(−)HDL-C					
At birth	23	23/25	25 (5)	25 (1)	23 (7)
3–4 M	60	41/44	48 (8)	46 (11)	45 (6)
12 M	58	50/53	51 (8)	48 (13)	47 (10)
LDL-C/HDL-C					
At birth	0.16	0.41/0.36	0.45 (0.11)[c]	0.67 (0.12)	0.76 (0.24)
3–4 M	0.36	0.74/0.87	0.94 (0.19)[c]	1.41 (0.24)	1.38 (0.33)
12 M	0.41	1.00/1.00	1.09 (0.25)[c]	1.45 (0.32)	1.45 (0.41)
Apo A-I					
At birth	80	75/86	85 (14)	84 (19)	78 (14)
3–4 M	150	109/113	120 (12)	123 (22)	122 (15)
12 M	145	121/122	124 (10)	121 (16)	120 (14)
Apo A-II					
At birth	16	16/17	18 (4)	19 (4)	17 (3)
3–4 M	30	18/22	25 (3)	26 (6)	23 (4)
12 M	29	22/22	25 (4)	26 (6)	25 (6)
Apo B					
At birth	10	13/13	16 (5)[a]	20 (6)	18 (5)
3–4 M	36	57/62	59 (11)[b]	74 (16)	74 (14)
12 M	38	57/67	64 (15)[a]	81 (17)	77 (16)
Apo E					
At birth	6.7	3.7/4.4	4.9 (0.8)	4.6 (1.2)	4.6 (1.2)
3–4 M	13.3	8.3/8.0	6.6 (1.3)[b]	4.7 (1.4)	4.9 (1.2)
12 M	14.4	6.7/5.8	6.3 (1.7)[c]	4.6 (1.4)	4.7 (1.2)

Data are presented as the range or mean (±SD).
Concentrations of lipids and apolipoproteins are expressed as mg/dl.
Gest. P, gestation period; TC, total cholesterol; TG, triglyceride; LDL-C, low-density lipoprotein-cholesterol; HDL-C, high-density lipoprotein-cholesterol; Apo E(+) HDL-C, apo E- rich HDL-C; ApoE(−) HDL-C, apo E- poor HDL-C; CETP, cholesteryl ester transfer protein.
[a] $p<0.05$.
[b] $p<0.01$.
[c] $p<0.001$ vs. non-affected siblings and age-matched controls.

3.2. Lipid, apolipoprotein, and CETP mass levels

As compared with non-affected siblings and healthy controls (non-affected groups), the compound heterozygote exhibited extremely

low CETP mass levels. In the I14A and D442G heterozygotes, CETP mass levels were about one-third and two-thirds of the level in the non-affected groups, respectively, during the first year of life (Table 1). In all groups, CETP mass levels were highest at birth, were slightly lower at 3–4 months, and remained constant at 12 months.

From birth to 12 months of age, the TC, LDL-C, and apoB levels were always low in the CETP-deficient groups, particularly in the compound heterozygote, compared with the non-affected groups. These levels in the two I14A heterozygotes were always similar to those in the D442G heterozygotes. The TG levels were similar among the groups throughout the study period, although they did not increase to the levels found in the compound heterozygote at 3–4 and 12 months. In the D442G heterozygous and non-affected groups, the TC, LDL-C, and apoB levels increased markedly during the first 3–4 months ($p<0.001$), although the increases in the D442G heterozygous group were significantly smaller than those in the non-affected groups (TC, $p<0.01$; LDL-C and apoB, $p<0.001$). After 3–4 months, significant increases were observed in the D442G heterozygous group ($p<0.01$) but not in the non-affected groups ($p>0.05$).

Total HDL-C levels at birth were similar among the groups. After 3–4 months, the D442G heterozygous group showed a high total HDL-C level compared with the levels in the two non-affected groups ($p<0.05$). In these 3 groups, the total HDL-C levels increased markedly during the first 3–4 months ($p<0.001$), with a larger increase in the D442G heterozygous group than in the non-affected groups ($p<0.01$). The greatest increase in total HDL-C and the highest level measured occurred in the compound heterozygote at 3–4 months (Table 1). After 3–4 months, no significant increases were observed in any of the groups. The total HDL-C levels in the 2 I14A heterozygotes were always similar to the level in the D442G heterozygotes.

ApoE-rich HDL-C changed characteristically, depending on the CETP genotype (Table 1). At birth, apoE-rich HDL-C levels were similar among the groups. After birth, apoE-rich HDL-C increased persistently in the compound heterozygote and decreased slightly in the non-affected groups. In the I14A or D442G heterozygotes, apoE-rich HDL-C changed in an inverse U-shape. In contrast, apoE-poor HDL-C levels changed similarly in all groups, with a doubling during the first 3–4 months ($p<0.001$) and no significant increase thereafter ($p>0.05$). With the exception of the compound heterozygote, who showed the high concentrations after 3–4 months, the absolute concentrations were nearly the same among the groups throughout the first year. The apo A-I and apo A-II levels tended to reflect the changes in apoE-poor HDL-C, while the apoE levels were reflective of apoE-rich HDL-C.

No gender differences were observed in the measured parameters in any of the groups. Furthermore, the genotypes of the mothers did not influence the parameter levels in heterozygous children or their non-affected siblings (data not shown).

3.3. Correlations between CETP mass and lipid levels

In heterozygous CETP-deficient subjects, LDL-C and HDL-C levels were closely related to the CETP mass levels. The LDL-C level always correlated positively with the CETP mass level (Fig. 1, open circles in the left panels). Total HDL-C and CETP mass levels showed a significant positive correlation at birth but a negative correlation at 3–4 and 12 months (Fig. 1, closed circles in the left panels). In healthy babies, neither the LDL-C level nor total HDL-C level correlated with the CETP mass level during the study period (Fig. 1, right panels).

In heterozygous CETP-deficient subjects, the correlation of apoE-poor HDL-C with CETP mass was positive at birth, non-significant at 3–4 months, and negative at 12 months (Fig. 2, closed circles in the left panels). ApoE-rich HDL-C showed no significant correlation with CETP mass at birth, but demonstrated strong inverse correlations with CETP mass levels at 3–4 and 12 months (Fig. 2, open circles in the left panels). In healthy babies, apoE-poor and apoE-rich HDL-C levels were not significantly correlated with CETP mass levels (Fig. 2, right panels).

We consistently found significant positive correlations between the LDL-C/HDL-C ratio and CETP mass from birth to 12 months in heterozygous CETP-deficient subjects. The regression line was much steeper at 3–4 and 12 months than at birth (Fig. 3, left panels). No significant correlation was observed in healthy babies.

4. Discussion

The present findings clearly indicate that CETP is a determinant for LDL-C and HDL-C in CETP deficiency in the first year of life. We found that CETP mass consistently exhibited a positive correlation with LDL-C from birth to 12 months in children with heterozygous CETP deficiency (Fig. 1, open circles of the left panels). In contrast, CETP mass had a positive correlation with HDL-C at birth and a negative correlation with HDL-C at 3–4 and 12 months (Fig. 1, closed circles of the left panels). Significant correlations of CETP mass with LDL-C and HDL-C were not observed in healthy control children.

Of note, D442G and I14A heterozygotes showed markedly low LDL-C levels during the first years of life. Several earlier studies of Asian children showed that the LDL level in D442G or I14A heterozygotes was not different from that in non-mutant healthy children [12,13]. In contrast, Japanese adults with heterozygous D442G or I14A mutations have been shown to have higher LDL-C levels [8,9]. Concerning LDL-C levels in subjects with the homozygous or compound heterozygous mutation, Nagano et al. reported that both I14A homozygotes (which have no CETP activity) and compound I14A and D442G heterozygotes

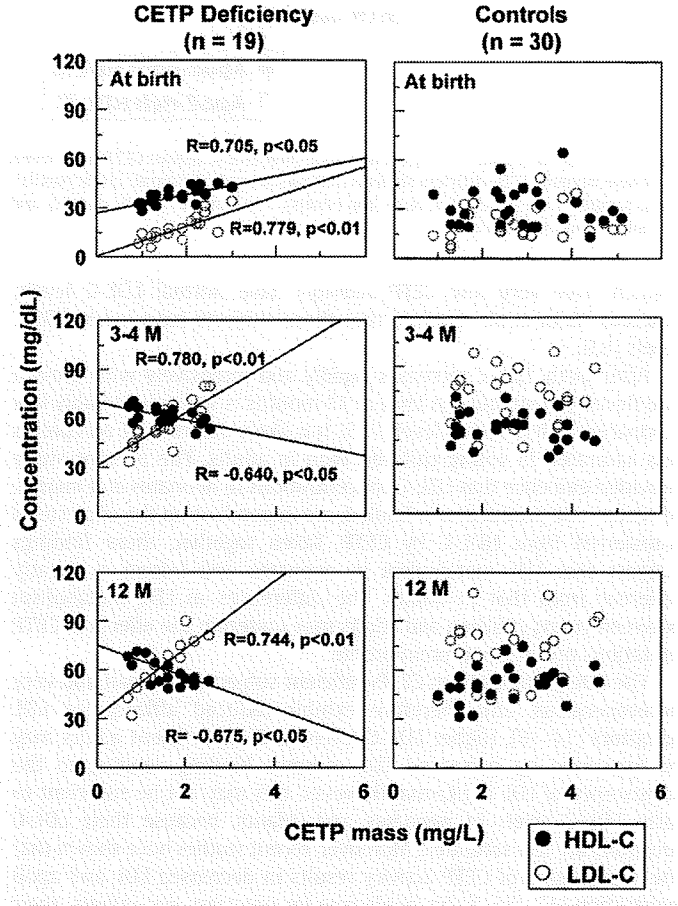

Fig. 1. Scatterplots of LDL-C and total HDL-C against CETP mass levels in 19 heterozygous CETP-deficient subjects (left panels) and 30 controls (right panels). The children with CETP deficiency consisted of 17 D442G and 2 I14A heterozygotes. Blood samples were obtained at birth (top panels), 3–4 months (middle panels), and 12 months (bottom panels).